Interfacing superconducting qubits and single optical photons

Sumanta Das[1], Sanli Faez[2] and Anders S. Sørensen[1]
[1]*Niels Bohr Institute, University of Copenhagen, Blegdamsvej 17, 2100 Copenhagen Ø, Denmark*
[2]*Debye Institute for Nanomaterials Science and Center for Extreme Matter and Emergent Phenomena, Utrecht University, Utrecht, The Netherlands*
(Dated: July 22, 2016)

We propose an efficient light-matter interface at optical frequencies between a superconducting qubit and a single photon. The desired interface is based on a hybrid architecture composed of an organic molecule embedded inside an optical waveguide and electrically coupled to a superconducting qubit far from the optical axis. We show that high fidelity, photon-mediated, entanglement between distant superconducting qubits can be achieved with incident pulses at the single photon level. Such low light level is highly sought for to overcome the decoherence of the superconducting qubit caused by absorption of optical photons.

PACS numbers: 03.67.-a, 42.50.Ex, 85.25.Cp

Over the past few years, rapid progress in engineering and control of their physical properties, have made superconducting (SC) qubits, one of the most promising candidates for future quantum processors [1–4]. To use such processors in quantum communication protocols and beyond, it is a necessity to build light-matter interfaces at optical frequencies, since quantum communication over long distances needs to be performed through optical fibers [5, 6]. This has stimulated immense interest in devising ways of efficiently coupling optical photons to SC systems [7–22]. Some success have been achieved in this regards, at microwave frequencies [23, 24], while in the optical domain, only limited indirect coupling have been achieved using transducers [25–27]. Coherent coupling of quantum fields at optical frequencies to a SC system thus remains an outstanding challenge. A principle obstacle to this is the large mismatch between the energy scales of an optical photon ($\sim$ 1 eV) and a SC qubit ($\sim$ 100 μeV) [23] making the absorption of even a single optical photon a major disturbance for a SC system.

In this letter we propose a scheme to *interface optical photons with a SC qubit* at light levels involving only a single or a few photons. To achieve this we introduce a hybrid solid-state architecture Fig.1(a) comprising, a dipole emitter embedded in an optical waveguide with a SC qubit fabricated near it. The individual components of this hybrid has already been realized. In comparison to the magnetic coupling, considered in numerous approaches to hybrid structures [16–18, 24, 28–33] a key feature of our scheme is the electric coupling between the emitter and SC qubit. The coupling strength can then be orders of magnitude stronger thus allowing for strong coupling in the system. To understand the physics of such electrical coupling let us consider the SC qubit to be a cooper pair box (CPB). As a cooper pair oscillates between the superconducting islands, it generates a variation in the electric field at the emitter. If the emitter has a large difference in the dipole moment between its ground and excited states, the electric field variation will lead to different Stark shift of the excited and ground energy levels (Fig.1 c). This leads to a sizeable shift of the resonance frequency of the emitter, which can be larger than its linewidth, leading to coherent coupling of the emitter and the qubit.

Since the emitter is in a waveguide, the shift can lead to measurable effects even for light pulses containing few photons resulting in minimal decoherence due to light fields. This is a major advantage over existing hybrid proposals that requires strong optical fields [2, 7, 19, 21, 24, 28–33], which is likely to be a major source of decoherence. We show how the achieved light-matter interface allows efficient optical readout of the qubit state. Furthermore, we put forward a detailed scheme for photon-mediated entanglement between two distant SC qubits. As a first example towards realization of such entanglement we discuss the generation of quantum correlation between an optical photon and a SC qubit, which shows violation of the Clauser-Horn-Shimony-Holt (CHSH) inequality.

The Hybrid: Our hybrid system consist of three elements shown schematically in Fig. 1 (a), an optical waveguide, a SC qubit fabricated near the waveguide's surface ($\sim 300 - 500$ nm) and a dipole emitter embedded in an organic matrix inside the waveguide. In addition to differential Stark shift, we assume that the emitter has an optical transition with a narrow linewidth as demonstrated for organic dye molecules [34, 35]. Placing an ideal two level emitter in an optical waveguide, in principle, allows for coupling efficiencies to optical photons of more than 95% [36, 37]. In practise however, given that the molecular electronic configuration involves several levels, the coupling may be smaller. For the applications we are concerned with here, a coupling efficiency of about 10% will be sufficient to achieve operations with few photons per pulse ($\lesssim 10$).

A typical CPB, with the gate charge $n_{\rm g}$ restricted to the range $[0, 1]$, only have one Cooper pair shared between the SC islands. The CPB thus resembles a two level system (Fig.1 b) which can be coherently manipulated at temperatures ≤ 100 mK [38, 39]. The Hamiltonian of this two level system can be written as $\mathcal{H}_{\rm cp} = -\frac{1}{2}(\chi_1\eta^{\rm z}+\chi_2\eta_{\rm x})$, where $\chi_1 \propto E_{\rm c}(1-2n_{\rm g})$, $\chi_2 \propto E_{\rm J}$, and $\eta^{\rm z}, \eta_{\rm x}$ are the Pauli spin-$1/2$ operators defined in the spin basis $\{|\uparrow\rangle, |\downarrow\rangle\}$ corresponding to the CPB charge states $\{0, 1\}$ [38, 39]. Here $E_{\rm c}$ and $E_{\rm J}$ are the Coulumb energy of an extra pair of charges on the island and the Josephson

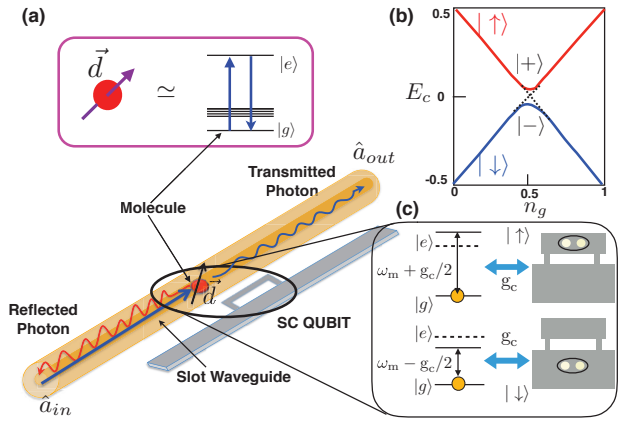

FIG. 1. Schematic of the hybrid molecule-SC system. (a) An organic molecule located inside the optical waveguide is electrically coupled to a SC via a Stark shift. Incident probe photons in the waveguide are scattered by the $0-0$ optical transition of the molecule. Due to the coupling of the SC qubit and the molecule, reflected and transmitted photons are entangled with the internal state of the qubit. (b) The energy levels of a SC qubit can be represented by two hybridized levels for a gate charge restricted in the range 0 to 1. (c) Oscillation of the cooper pair between the SC island leads to shift of the molecular resonance.

energy respectively. The Hamiltonian of the molecule-qubit hybrid can be written in the form, $\mathcal{H} = \mathcal{H}_0 + \mathcal{H}_{\rm I}$, where $\mathcal{H}_0$ is the free energy part of the Hamiltonian containing the molecular, field and CPB energies [40], while $\mathcal{H}_{\rm I}$ is the interaction Hamiltonian governing the coherent dynamics,

$$\mathcal{H}_{\rm I} = \frac{\hbar {\rm g_m}}{2}\sigma^{+}\hat{a}e^{-i\omega_{\rm p}t} + {\rm H.c.} + \frac{1}{4}\hbar {\rm g_c}\eta^{\rm z}\otimes(\sigma^{\rm z}+\mathbb{I})\,. \quad (1)$$

Here the first and the third term corresponds respectively to the light-molecule and molecule-CPB interactions. The operators $\sigma^z, \sigma^{\pm}$ for the molecule are the standard dipole transition operators for a two level system and $\hat{a}$ is the field operator of the incoming photon pulse [41] of central frequency $\omega_{\rm p}$. The incoming light couples to the molecule with a strength ${\rm g_m} = \wp_{\rm eg}\cdot\mathcal{F}/\hbar$, where $\wp_{\rm eg}$ is the dipole moment of the optical transition $|e\rangle \leftrightarrow |g\rangle$ in the molecule and $\mathcal{F}$ the mode function of the incoming photon in the one-dimensional waveguide. Furthermore, ${\rm g_c} = \Delta\wp_{\rm c}\cdot\Delta\mathcal{E}/\hbar$ is the molecule-CPB coupling strength, where $\Delta\wp_{\rm c}$ is the difference in the static dipole moments between the excited and ground manifold of the molecule, while $\Delta\mathcal{E}$ is the electrostatic field variation as seen by the molecule due to the tunnelling of a single Cooper pair.

Qubit state detection: We first outline a recipe for detecting the qubit's state by optical photons. We assume that the CPB is operated at a gate voltage away from the sweet spot $(n_{\rm g} \neq 1/2)$ in the linear regime of Fig. 1 (b). Working in this regime, the eigenstates of the qubit Hamiltonian $\mathcal{H}_{\rm cp}$ are the $\eta^{\rm z}$ eigenstates. The CPB-molecule interaction Hamiltonian (1) reveals that the state of the qubit shifts the excited state of the molecule by $\pm\frac{1}{2}\hbar{\rm g_c}$, compared to the unperturbed resonance at $\omega_{\rm m}$ (Fig. 1 c) making it sensitive to the qubit state. The molecular resonance line is then split into two, such that, the position of each line corresponds to one of the qubit states $\{|\uparrow\rangle, |\downarrow\rangle\}$, with the splitting given by the molecule-qubit coupling ${\rm g_c}$. We can therefore determine the state of the qubit by studying the scattering of an incoming photons and measuring whether they are transmitted or reflected.

To describe the protocol we consider the Hamiltonian $\mathcal{H}_I$ (1) and evaluate the photon scattering amplitudes $\zeta_{\uparrow,\downarrow}$ of input photons, for the qubit states $|\uparrow\rangle$ and $|\downarrow\rangle$ assuming that we are below saturation. We do this using an effective operator formalism [1] generalized to Heisenberg picture [40]. We find the amplitude of the reflected field $\hat{a}_{o,\uparrow(\downarrow)}$ corresponding to the qubit state $|\uparrow\rangle(|\downarrow\rangle)$ to be,

$$\hat{a}_{o,\uparrow(\downarrow)} = i\zeta_{\uparrow(\downarrow)}\hat{a}_{\rm in} = i\left(\frac{\gamma_{1D}}{2}\right)\left[\Delta - i\gamma/2 \underset{(-)}{+} {\rm g_c}/2\right]^{-1}\hat{a}_{\rm in}, \quad (2)$$

where, γ_{1D} is the rate of decay of the emitter into the one-dimensional waveguide mode, $\Delta = \omega_p - \omega_m$ is the detuning from the molecular resonance, γ is the total decay of the molecules and $\hat{a}_{in}$ represent the input quantum field (the incoming photon). From Eq. (2) we find two different resonance conditions $\Delta = \pm\frac{1}{2}{\rm g_c}$, for the respective qubit states $|\uparrow\rangle$ and $|\downarrow\rangle$.

A simple numerical estimate gives an electrostatic field variation of roughly $\Delta\mathcal{E} = (2.5-8)$ kV/m, at the location of the molecule for a waveguide of permitivity ~ 4.7, due to presence of a cooper pair on an island situated about $\sim (500-300)$ nm away [43]. Hence, for $\Delta\wp_{\rm c} = 1$ D [34, 44, 45], we can obtain a coupling strength of ${\rm g_c} \sim (2\pi)\times(25-80)$ MHz. As an organic molecule typically has a line width $\gamma \sim (2\pi)\times 20$ MHz [34, 45], we can thus achieve strong coupling in the hybrid system. Since the separation between the resonance peaks is larger than their width ${\rm g_c} > \gamma$, we can distinguish between the two internal states of the qubit by sending in a single photon pulse resonant with one of the peaks and measuring whether photons are reflected. At resonance we evaluate the reflection probability to be $(\gamma_{1D}/\gamma)^2$, so that we can distinguish the two state by sending in $(\gamma/\gamma_{1D})^2 \sim 100$ photons even for a conservative estimate of $\gamma_{1D}/\gamma = 0.1$ [35].

The above depicted scheme may allow efficient optical readout of SC qubits. A more promising application however, would be a coherent interface. As a first example of this, we discuss an entanglement protocol. To minimize the decoherence arising due to charge noise [46, 47] it is necessary to operate the qubit near the sweet spot of the CPB ($\chi_1 = 0$) to achieve coherent operation. At this point, $\langle+|\eta^z|+\rangle = \langle-|\eta^z|-\rangle = 0$, and the CPB-molecule coupling term in the Hamiltonian contributes only to the second order, and would therefor require strong light fields, see details in [40].

To be able to work with a single to few photons an alternative is to consider, a *Raman scattering scheme* as shown in

Fig. S4 (a). This is realized, by having two organic molecules with properties as above and with optical transitions of nearly the same frequencies, e.g., achieved by tuning them into resonance using an external field [48]. The molecules are assumed to have a separation less than the optical wavelength, and thus couple to each other via near field optical dipolar interaction. Furthermore, we assume a reflector at one end of the waveguide such that the waveguide is single sided to maximize the collection of Raman photons. The Hamiltonian can then be written as $\mathcal{H} = \mathcal{H}_0 + \mathcal{H}_{\rm dd} + \mathcal{H}_{\rm I}$. Here, $\mathcal{H}_0$ is free energy part having contribution from both molecules and the qubit [40], $\mathcal{H}_{\rm dd} = \hbar {\rm V}(\sigma_1^+\sigma_2^- + \sigma_2^+\sigma_1^-)$ is the dipolar coupling Hamiltonian of strength V, while the interaction Hamiltonian is,

$$\mathcal{H}_{\rm I} = \sum_j \left[\frac{\hbar {\rm g}_{{\rm m}_j}}{2} \sigma_j^+ \hat{a} e^{-i\omega_{\rm p} t} + {\rm H.c.} + \frac{\hbar {\rm g}_{{\rm c}_j}}{4} \eta^{\rm z} \otimes \left(\sigma_j^{\rm z} + \mathbb{I}\right) \right], \tag{3}$$

where ${\rm g}_{{\rm m}_j}$ and ${\rm g}_{{\rm c}_j}$ for $(j = 1, 2)$ corresponds to the coupling strength of the incoming light and CPB to the molecules respectively. The strong dipole-dipole interaction $\mathcal{H}_{\rm dd}$ can be diagonalized to form two dressed state $|S\rangle$ and $|A\rangle$ which are split by $2\mathcal{V} = \sqrt{4{\rm V}^2 + \delta_0^2}$. Using an external field to vary the difference in the molecular energies $\delta_0 = (\omega_1 - \omega_2)$, the transition between the dressed states can be brought into resonance with the qubit transition, $2\mathcal{V} = \omega_{\rm q}$. This resonance condition allows the exchange of energy between the qubit and the excited manifold of the molecules which enables the Raman transition $|g,-\rangle \rightarrow |S,-\rangle \rightarrow |A,+\rangle \rightarrow |g,+\rangle$ (Fig. S4 a). Here the molecular system starts and ends in the joint ground state $|g\rangle = |g_1, g_2\rangle$ while the qubit is flipped from state $|-\rangle$ to $|+\rangle$ by the emission of a Stokes photon of frequency $\omega_{\rm s} = (\omega_{\rm p} - \omega_{\rm q})$. The effective coupling constant between the states $|S,-\rangle$ and $|A,+\rangle$ which enables this transition is given by $\mathcal{G} = ({\rm g}_{{\rm c}_1} - {\rm g}_{{\rm c}_2}){\rm V}/\sqrt{4{\rm V}^2 + \delta_0^2}$. Using the same formalism as above, we find that at resonance the probability for an incident single photon to induce a Raman scattering into the waveguide, for moderate coupling ${\rm g}_{{\rm c}_{1,2}}^2/\gamma\omega_{\rm q} < 1$ is $\mathcal{P}_R = (\gamma_{1D}/\gamma)^2 \wp_R$, where [40],

$$\wp_R = \left(\frac{\delta_0}{\omega_{\rm q}}\right)^2 \left(\frac{4\mathcal{G}^2}{\Gamma_s^2\Gamma_a^2/4\gamma^2 + 4\mathcal{G}^2}\right). \tag{4}$$

Here $\gamma = \gamma_{1D} + \gamma_c + \gamma^i$ is the total decay rate of each molecule (assumed to be same for both the molecules), $\Gamma_s = \gamma + 2\gamma_c {\rm V}/\omega_{\rm q}, \Gamma_a = \gamma - 2\gamma_c {\rm V}/\omega_{\rm q}$ are the decay rates of the states $|S\rangle$ and $|A\rangle$ respectively, γ^i is the intrinsic decay rate of each molecule while γ_c is the collective decay rate of the molecules. In deriving the Raman scattering probability we assumed that the molecules have the same γ_{1D} and that they are close enough so that we can ignore effects of phases in the collective decay [49] arising from the spatial positions of the molecules. The probability of Raman scattering is much larger than the reverse process $|A,+\rangle \rightarrow |S,-\rangle$, which is suppressed by a factor $(\mathcal{G}\gamma)^2/\omega_{\rm q}^4$ since it is off resonant [40].

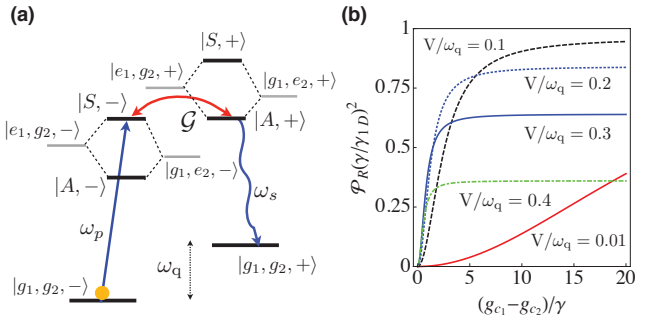

FIG. 2. (a) Schematics of Raman configuration. The molecular levels $|e_1 g_2\rangle$ and $|g_1 e_2\rangle$ are hybridized by the dipole-dipole interaction to form the dressed states $|A\rangle$ and $|S\rangle$, the separation of which is tuned into resonance with the qubit frequency $\omega_{\rm q}$. A photon scattered along the transition $|g,-\rangle \rightarrow |S,-\rangle$ is emitted as a Stokes photon along the transition $|A,+\rangle \rightarrow |g,+\rangle$ due to resonant coupling among the states $|S,-\rangle \leftrightarrow |A,+\rangle$. (b) Probability of Raman scattering into the waveguide for a single incident photon as a function of coupling $({\rm g}_{{\rm c}_1} - {\rm g}_{{\rm c}_2})/\gamma$ for different values of the dipolar coupling strength. Here we have assumed $\gamma_c/\gamma = 0.45$

In Fig. S4 (b) we plot the Raman probability as a function of $\left({\rm g}_{{\rm c}_1} - {\rm g}_{{\rm c}_2}\right)/\gamma$ for different values of the ratio between the dipolar coupling and qubit frequency ${\rm V}/\omega_q$. The results can be understood from the need to have both good hybridization and coupling to the waveguide. For low ${\rm V}/\omega_q$ the hybridization of $|e_1 g_2\rangle$ and $|g_2 e_1\rangle$ to $|A\rangle$ and $|S\rangle$ is small which limits the coupling, whereas for ${\rm V}/\omega_q \rightarrow 1/2$, $\delta_0 \rightarrow 0$, $|A\rangle$ becomes a dark state of the coupling to the waveguide so that $\mathcal{P}_R \rightarrow 0$. For ${\rm V}/\omega_{\rm q} \gtrsim 0.1$, the probability quickly reaches its maximum value even for limited coupling strengths $({\rm g}_{{\rm c}_1} - {\rm g}_{{\rm c}_2})/\gamma \gtrsim 1$, whereas saturation is slower for weaker dipole coupling due to the lack of hybridization. We find from Fig. S4 (b), that for a feasible ${\rm V}/\omega_{\rm q} = 0.1$ and even a moderate coupling strength of $({\rm g}_{{\rm c}_1} - {\rm g}_{{\rm c}_2})/\gamma = 5$, the Raman scattering probability takes a value $\mathcal{P}_R \simeq 0.77 \times (\gamma_{1D}/\gamma)^2$. This set of parameters will be used for all numerical examples. The value of $\mathcal{P}_R$, is close to its upper limit of $(\gamma_{1D}/\gamma)^2$ set by the necessity of having both waveguide absorption and emission by the emitter. Furthermore, the Raman probability is not very sensitive to the precise value of the dipole coupling making it attractive even for randomly placed molecules.

The effective Raman scheme, allows the use of the interferometric framework [50, 51], shown schematically in Fig. 3 (a) to generate entanglement between distant SC qubits via the detection of a photon. For this purpose we assume that both hybrids are initialized in state $|g,-\rangle_{1(2)}$. Scattering of an incoming single photon pulse off the hybrids, followed by a beam splitter which erases the which way information then creates one of the maximally entangled Bell states $|\Psi_\pm\rangle = \frac{1}{\sqrt{2}}|g\rangle\left(|-\rangle_1|+\rangle_2 \pm |+\rangle_1|-\rangle_2\right)$ conditioned on the detection of a photon in the detectors $D_\pm$ after frequency filtering out photons which have not undergone a Raman scattering.

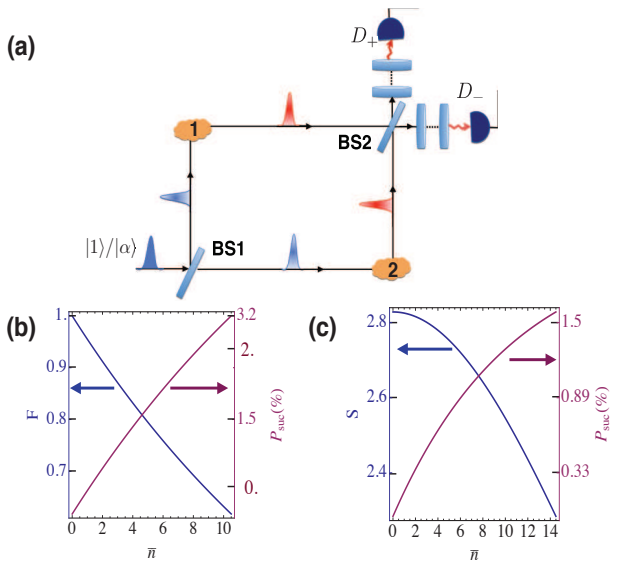

FIG. 3. (a) Interferometric scheme to generate maximally entangled Bell state $|\Psi_+\rangle$ between two SC qubits using a single photon $|1\rangle$ or coherent state $|\alpha\rangle$ as input. Generation of entanglement is conditioned on a click of detector $D_\pm$. (b) Fidelity F and success probability $P_{\rm suc}^{(c)}$ as a function of mean number of photons in the incoming pulse for Bell state generation. (c) Bell parameter S and success probability $P_{\rm suc}^{(c)}$ as a function of mean number of photons in the incoming pulse for an entangled state between a single qubit and a photon. For all the plots we have assumed $\gamma_{1D}/\gamma = 0.1$, $\eta = 50\%$, $(\mathrm{g}_{c_1} - \mathrm{g}_{c_2})/\gamma = 5$, $\mathcal{P}_R = 0.77 \times (\gamma_{1D}/\gamma)^2$ and $\gamma_c/\gamma = \gamma^i/\gamma = 0.45$

To describe these processes we again use the input-output formalism [40]. For simplicity we consider the two hybrids to have equivalent physical properties and work in the limit of moderate coupling $\mathrm{g}_{c_{1,2}}^2/\gamma\omega_{\rm q} < 1$. Assuming the input pulse to be a single photon, we find that the process has a fidelity $F = 1$, and a success probability of $P_{\rm suc}^{(1)} = \eta\mathcal{P}_R$, where η is the photodetection efficiency of the single photon detectors. For a moderate molecule-qubit coupling strength $(\mathrm{g}_{c_1} - \mathrm{g}_{c_2})/\gamma = 5$, and the set of parameters used above along with $\gamma_{1D}/\gamma = 0.1$, we get $P_{\rm suc}^{(1)} \simeq 3.8 \times 10^{-3}$, for $\eta = 50\%$.

The above mentioned success probability can be improved by considering a weak coherent state as input. Assuming identical hybrids and an intensity below saturation, we find the conditional fidelity to be $F = 1 - (1 + \mathcal{P}_{RO}/\mathcal{P}_R)\, P_{\rm suc}^{(c)}/\eta$, with the corresponding success probability [40]

$$P_{\rm suc}^{(c)} = P_{\rm suc}^{(1)} \left\{ \frac{1 - e^{-\bar{n}(\mathcal{P}_R + \mathcal{P}_{RO})}}{\mathcal{P}_R + \mathcal{P}_{RO}} \right\}, \qquad (5)$$

where $\bar{n}$ is the mean number of photons in the incident pulse and the probability of Raman scattering to the outside (not into the mode of the waveguide) is $\mathcal{P}_{RO} = \left(\frac{\gamma_{1D}}{\gamma}\right)\left\{\left(\frac{\gamma_c}{\gamma}\right)\left(\frac{\delta_0}{\omega_{\rm q}}\right)^2 + \left(\frac{\gamma^i}{\gamma}\right)\left(1 + \frac{2V}{\omega_{\rm q}}\right)\right\}\left(\frac{2\mathcal{G}^2}{\Gamma_s^2\Gamma_a^2/4\gamma^2 + 4\mathcal{G}^2}\right)$. As an example, for $\bar{n} = 1.5$ we get a success probability $P_{suc}^{(c)} \simeq 5.5 \times 10^{-3}$ for creating a Bell state with fidelity $F \sim 93\%$. Thus for an input coherent state, we gain substantially in experimental simplicity with limited reduction in fidelity. We show in Fig. S4 (b), the behavior of F and $P_{\rm suc}^{(c)}$ as a function of the mean photon numbers.

The above two qubit entanglement protocol can serve as building block of a quantum network. A first step in this direction can be achieved with a much simpler entanglement protocol between a single qubit (CPB) and a photon. For this purpose, we consider an interferometer similar to Fig. 3(a) with the hybrid 1 replaced by a frequency modulator shifting the frequency by $\omega_{\rm q}$. The hybrid is assumed to be initialized in state $|g, -\rangle$. In this case upon post selecting a photon at one of the detectors, the combined state of a photon and hybrid becomes $|\Psi_{\rm s}^+\rangle = \frac{1}{\sqrt{2}}\left(|U_k\rangle|g,-\rangle + |L_k\rangle|g,+\rangle\right)$, where $|U_k\rangle$ and $|L_k\rangle$ represent respectively a photon in the upper and lower arm of the interferometer. To verify this, we consider violation of the CHSH inequality $S \leq 2$ [5, 6] between the qubit and photon. We find for a coherent state input, by properly balancing the interferometer after inserting a phase Φ in one of its arm and measuring the qubit in a suitable basis, a violation of the CHSH inequality [40]

$$S = 2\sqrt{2}\left[\frac{2e^{-\bar{n}(\mathcal{P}_R + \mathcal{P}_{RO})}}{1 + e^{-\bar{n}(\mathcal{P}_R + \mathcal{P}_{RO})}}\right], \qquad (6)$$

with a success probability $P_{\rm suc}^{(c)} = \frac{1}{2}P_{\rm suc}^{(1)}\left(\mathcal{P}_R + \mathcal{P}_{RO}\right)^{-1}\left(1 - e^{-2\bar{n}[\mathcal{P}_R + \mathcal{P}_{RO}]}\right)$. In Fig. 3 (c) we show the behavior of S and $P_{\rm suc}^{(c)}$ as a function of the mean photon number. Using the above parameters we find $S > 2.5$ for $\bar{n} = 10$, with a corresponding success probability $P_{\rm suc}^{(c)} \simeq 1.3\%$ for $\eta = 50\%$.

So far we have ignored the time T it takes to perform the light scattering. To avoid decoherence, the scattering process needs to be completed within the coherence time of the qubit. Since we rely on resonance condition with states of width γ, the pulse duration needs to satisfy $\gamma T \gg 1$. With $\gamma = (2\pi)20$ MHz we can chose a pulse duration $T = 50$ ns which is still much shorter than typical coherence times of CPB (about 500 ns)[54]. Much better coherence times can be achieved if we replace the CPB with a transmon qubit where, $T_2 \sim 3\mu$s) [47]. For typical available size and coupling strengths of the transmon and CPB we estimate that the coupling to the molecule will be smaller for a transmon, $\mathrm{g}_{\rm c}^{\rm T} \sim \mathrm{g}_{\rm c}/6$ [47]. Using Eq. (4), we estimate that for a transmon with such coupling constant $[(\mathrm{g}_{c_1} - \mathrm{g}_{c_2})/\gamma]/6$ the probability of Raman scattering process is $\sim 0.1 \times (\gamma_{1D}/\gamma)^2$ which however can be improved by considering a larger dipole coupling $\mathrm{V}/\omega_{\rm q} > 0.1$. For instance, from Fig. S4(b) we estimate that when $\mathrm{V}/\omega_{\rm q} \sim 0.2$, $\mathcal{P}_R \sim 0.3 \times (\gamma_{1D}/\gamma)^2$. For such reduced Raman rate, we only suffer a minor decrease in the success probability for transmons but gain in terms of qubit coherence.

In conclusion we have proposed a novel hybrid system formed by an organic molecule embedded in a polymer matrix of an optical waveguide and electrically coupled to a SC

qubit, that provide a light-matter interface for quantum information transfer over long distances. In particular, our proposed schemes work at low light levels (single to few photons). This facilitates, the merger of optics with SC systems without severe detrimental effects, caused by optical absorption. Furthermore, as the component of the hybrid system are in solid state, it should be readily scalable and integrable with current technologies and optics. This could open new directions in quantum communication using SC quantum processors in an integrated circuitry with optical photons.

S.D and A. S gratefully acknowledge financial support from ERC Grant QIOS (Grant No. 306576) and the Danish council for independent research (Natural Sciences). SF acknowledges support by the European Research Council, Project No. 279248.

[1] R. J. Schoelkopf and S. M. Girvin, Nature **451**, 664 (2008).
[2] M. H. Devoret and R. J. Schoelkopf, Science **339**, 1169 (2013).
[3] J. Kelly, R. Barends, A. G. Fowler, A. Megrant, E. Jeffrey, T. C. White, D. Sank, J. Y. Mutus, B. Campbell, Yu Chen, Z. Chen, B. Chiaro, A. Dunsworth, I.-C. Hoi, C. Neill, P. J. J. O'Malley, C. Quintana, P. Roushan, A. Vainsencher, J. Wenner, A. N. Cleland and J. M. Martinis, Nature **519**, 66-69 (2015).
[4] A.D. Crcoles, E. Magesan, S. J. Srinivasan, A. W. Cross, M. Steffen, J. M. Gambetta and J. M. Chow, Nature Communications **6**, Article number: 6979 (2015).
[5] N. Gisin, G. Ribordy, W. Tittel, and H. Zbinden Rev. Mod. Phys. **74**, 145 (2002).
[6] H. J. Kimble, Nature **453**, 1023 (2008).
[7] A. S. Sørensen, C. H. van der Wal, L. I. Childress and M. D. Lukin, Phys. Rev. Lett. **92**, 063601 (2004).
[8] P. Rabl, D. DeMille, J. M. Doyle, M. D. Lukin, R. J. Schoelkopf and P. Zoller, Phys. Rev. Lett., **97**, 033003 (2006).
[9] A. Andre, D. DeMille, J. M. Doyle, M. D. Lukin, S. E. Maxwell, P. Rabl, R. J. Schoelkopf and P. Zoller, Nature Physics, **2**, 636 (2006).
[10] M. Wallquist, K. Hammerer, P. Rabl, M. Lukin, and P. Zoller, Phys. Scr. **T137**, 014001 (2009).
[11] J. M. Taylor, A. S. Sørensen, C. M. Marcus, and E. S. Polzik, Phys. Rev. Lett. **107**, 273601 (2011).
[12] S. Barzanjeh, M. Abdi, G. J. Milburn, P. Tombesi, and D. Vitali, Phys. Rev. Lett. **109**, 130503 (2012).
[13] L. Tian, Phys. Rev. Lett. **108**, 153604 (2012).
[14] Y.-D. Wang and A. A. Clerk, Phys. Rev. Lett. **108**, 153603 (2012).
[15] Z-L. Xiang, S. Ashhab, J. Q. You, and F. Nori, Rev. Mod. Phys. **85**, 623 (2013).
[16] D. Marcos, M. Wubs, J. M. Taylor, R. Aguado, M. D. Lukin and A. S. Sørensen, Phys. Rev. Lett., **105**, 210501 (2010).
[17] K. Xia, M. R. Vanner and J. Twamley, Sci. Rep. **4**, 5571 (2014).
[18] C. OBrien, N. Lauk, S. Blum, G. Morigi, and M. Fleischhauer Phys. Rev. Lett. **113**, 063603 (2014).
[19] J. D. Pritchard, J. A. Isaacs, M. A. Beck, R. McDermott, and M. Saffman Phys. Rev. A **89**, 010301 (2014).
[20] L. A. Williamson, Y.-H. Chen, and J. J. Longdell, Phys. Rev. Lett. **113**, 203601 (2014).
[21] Z. Q. Yin, W. L. Yang, L. Sun, L. M. Duan, Phys. Rev. A **91**, 012333 (2015).
[22] Ondrej Cernotik and Kl. Hammerer, arXiv:1512.00768 (2015).
[23] A. Wallraff, D. I. Schuster, A. Blais, L. Frunzio, R.- S. Huang, J. Majer, S. Kumar, S. M. Girvin and R. J. Schoelkopf, Nature **431**,162 (2004).
[24] Y. Kubo, F. R. Ong, P. Bertet, D. Vion, V. Jacques, D. Zheng, A. Dréau, J.-F. Roch, A. Auffeves, F. Jelezko, J. Wrachtrup, M. F. Barthe, P. Bergonzo, and D. Esteve, Phys. Rev. Lett. **105**, 140502 (2010).
[25] J. Bochmann, A. Vainsencher, D. D. Awschalom, and A. N. Cleland, Nature Physics **9**, 712 (2013).
[26] R. W. Andrews, R. W. Peterson, T. P. Purdy, K. Cicak, R. W. Simmonds, C. A. Regal, and K. W. Lehnert, Nature Physics **10**, 321 (2014).
[27] T. Bagci, A. Simonsen, S. Schmid, L. G. Villanueva, E. Zeuthen, J. Appel, J. Taylor, A. S. Sørensen, K. Usami, A. Schliesser, and E. S. Polzik, Nature **507**, 81 (2014).
[28] S. Probst, H. Rotzinger, S. Wünsch, P. Jung, M. Jerger, M. Siegel, A. V. Ustinov, and P. A. Bushev, Phys. Rev. Lett. **110**, 157001 (2013).
[29] D. I. Schuster, A. P. Sears, E. Ginossar, L. DiCarlo, L. Frunzio, J. J. L. Morton, H. Wu, G. A. D. Briggs, B. B. Buckley, D. D. Awschalom, and R. J. Schoelkopf, Phys. Rev. Lett. **105**, 140501 (2010).
[30] K. Tordrup and K. Mølmer, Phys. Rev. A **77**, 020301 (2008)
[31] A. Imamoğlu, Phys. Rev. Lett. **102**, 083602 (2009).
[32] J. Verdú, H. Zoubi, Ch. Koller, J. Majer, H. Ritsch, and J. Schmiedmayer, Phys. Rev. Lett. **103**, 043603 (2009);
[33] X. Zhu, S. Saito, A. Kemp, K. Kakuyanagi, S. Karimoto, H. Nakano, W. Munro, Y. Tokura, M. S. Everitt, K. Nemoto, M,Kasu, N. Mizuochi and K. Semba, Nature **478**, 221224 (2011)
[34] Y. L. A. Rezus, S. G. Walt, R. Lettow, A. Renn, G. Zumofen, S. Götzinger and V. Sandoghdar, Phys. Rev. Lett., **108**, 093601, (2012).
[35] S. Faez, P. Türschmann, H. R. Haakh, S. Götzinger and V. Sandoghdar, Phys. Rev. Lett. **113**, 213601 (2014).
[36] V. R. Almeida, Qianfan Xu, C. A. Barrios and M. Lipson, Optics Letters, **29**,1209 (2004).
[37] Q. Quan, I. Bulu and M. Lončar, Phys. Rev. A, **80**, 011810 (2009).
[38] Y. Makhlin, G. Schoen and A. Shnirman, Rev. Mod. Phys. **73**, 357 (2001).
[39] V. Bouchiat, D. Vion, P. Joyez, D. Esteve and M. H. Devoret Physica Scripta. **T76**, 165, (1998).
[40] See supplementary information for details.
[41] M. O. Scully and M. H. Zubairy, *Quantum Optics*, Cambridge University Press (1997).
[42] Florentin Reiter and Anders S. Sørensen, Phys. Rev. A, **85**, 032111 (2012).
[43] S.Faez, S. J. van der Molen, and M. Orrit, Physical Review B, **90**, 205405 (2014).
[44] M. Orrit, J. Bernard, A. Zumbusch, and R. I. Personov, Chem. Phys. Lett. **196**, 595 (1992).
[45] Ch. Brunel, Ph. Tamarat, B. Lounis, J. C. Woehl, and Michel Orrit, J. Phys. Chem. A **103**, 2429 (1999).
[46] G. Ithier, E. Collin, P. Joyez, P. J. Meeson, D. Vion, D. Esteve, F. Chiarello, A. Shnirman, Y. Makhlin, J. Schriefl, and G. Schön, Phys. Rev. B. **72**, 134519 (2005).
[47] A. A. Houck, J. Koch, M. H. Devoret, S. M. Girvin and R. J. Schoelkopf, Quantum Inf Process **8**, 105 (2009).
[48] C. Hettich, C. Schmitt, J. Zitzmann, S. Khn, I. Gerhardt, V. Sandoghdar, Science **298**, 385-389 (2002).
[49] S. Das, G.S. Agarwal, and M. O. Scully, Phys. Rev. Lett **101**, 153601 (2008).
[50] C. Cabrillo, J. I. Cirac, P. Garcia-Fernández and P. Zoller, Phys.

Rev. A, **59**, 1025 (1999).
[51] L. I. Childress, J. M. Taylor, A. S. Sørensen, and M. D. Lukin, Phys. Rev. A **72**, 052330 (2005).
[52] J. F. Clauser, M. A. Horne, A. Shimony, and R. A. Holt Phys. Rev. Lett. **23**, 880 (1969).
[53] A. Aspect, P. Grangier, and G. Roger Phys. Rev. Lett. **47**, 460 (1981).
[54] A. Wallraff, D. I. Schuster, A. Blais, L. Frunzio, J. Majer, M. H. Devoret, S. M. Girvin, and R. J. Schoelkopf Phys. Rev. Lett. **95**, 060501 (2005).

Supplementary Material: Interfacing superconducting qubits and single optical photons

SYSTEM HAMILTONIAN AND STATE DETECTION

Here we give the full system Hamiltonian and describe the details of the qubit detection scheme. The Hamiltonian of the combined molecule-CPB qubit hybrid system can be written as $\mathcal{H} = \mathcal{H}_0 + \mathcal{H}_{\rm I}$, where $\mathcal{H}_0 = \mathcal{H}_{\rm cp} + \mathcal{H}_{\rm m} + \mathcal{H}_{\rm f}$. Here $\mathcal{H}_{\rm cp} = \frac{1}{2}\left(\chi_1\eta^{\rm z} + \chi_2\eta_{\rm x}\right)$, is the free energy Hamiltonian of the qubit with $\chi_1 \propto E_{\rm c}(1-2n_{\rm g})$ and $\chi_2 \propto E_{\rm J}$, where $E_{\rm c}$ and $E_{\rm J}$ are defined in the main text. The gate charge n_g is defined by $n_g = C_g V_g/2e$, where, C_g and V_g are the gate capacitance and voltage respectively while e is the charge of an electron. In the charge regime (Josephson junction energy $E_{\rm J} \ll E_{\rm c}, n_g \neq 1/2$), the qubit states are eigenstate of the $\eta^{\rm z}$ Hamiltonian and hence the free energy Hamiltonian for the qubit becomes $\mathcal{H}_{\rm q} = \frac{1}{2}\hbar\omega_{\rm q}\eta^{\rm z}$ where $\omega_{\rm q}$ is the qubit transition frequency $\propto E_{\rm c}(1-2n_{\rm g})/\hbar$. The Hamiltonian $\mathcal{H}_{\rm m} = \frac{1}{2}\hbar\omega_{\rm m}\sigma^z$ is the free energy Hamiltonian of the molecule with $\omega_{\rm m}$ being the transition frequency of the optical dipole in the molecule and $\mathcal{H}_{\rm f} = \sum_{\rm k}\hbar\omega_{\rm k}(\hat{a}_{\rm k}^\dagger\hat{a}_{\rm k} + 1/2)$, is the free field Hamiltonian with $\hat{a}_{\rm k}$ being the field operator of mode k and frequency $\omega_{\rm k}$. The interaction Hamiltonian $\mathcal{H}_{\rm I}$ can be divided into two parts $\mathcal{H}^{\rm I}_{\text{m-L}}$ and $\mathcal{H}^{\rm I}_{\text{m-q}}$. The Hamiltonian $\mathcal{H}^{\rm I}_{\text{m-L}}$, describe the interaction between the incoming photon and the molecule and can be written

$$\mathcal{H}^{\rm I}_{\text{m-L}} = \frac{\hbar g_{\rm m}}{2}\sigma^+\hat{a}e^{i[kr-\omega_{\rm p}t]} + \frac{\hbar g_{\rm m}}{2}\hat{a}^\dagger\sigma^- e^{-[ikr-\omega_{\rm p}t]}. \tag{S7}$$

$\mathcal{H}^{I}_{\text{m-q}}$ is the interaction between the molecule and the SC qubit and has the structure

$$\mathcal{H}^{\rm I}_{\text{m-q}} = \frac{\hbar g_{\rm c}}{4}\eta^{\rm z}\otimes\left(\sigma^{\rm z} + \mathbb{I}\right), \tag{S8}$$

where $\eta^{\rm z} = (|\downarrow\rangle\langle\downarrow| - |\uparrow\rangle\langle\uparrow|)$, $\sigma^{\rm z} = (|e\rangle\langle e| - |g\rangle\langle g|)$, $\sigma^+ = |e\rangle\langle g|(\sigma^- = [\sigma^+]^\dagger)$. The couplings $g_{\rm m}$ and $g_{\rm c}$ are defined in the main text.

To investigate the effect of coupling between the molecule and the CPB, and to develop a scheme for the detection of the qubit state, we now study coherent scattering of optical photons from the hybrid system. Due to the light-matter interaction, the scattering maps the qubit state onto the scattered optical photons, and the detection of these then provide information about the qubit state. We here assume the CPB to be operated at a gate voltage away from the sweet spot ($n_g \neq 1/2$). The qubit levels are then given by the eigenstates $\{|\downarrow\rangle, |\uparrow\rangle\}$ of the operator $\eta^{\rm z}$. Furthermore, to study the dynamics of the hybrid, we choose a combined molecule-CPB qubit basis $\{|e,\downarrow\rangle, |e,\uparrow\rangle, |g,\downarrow\rangle, |g,\uparrow\rangle\}$ and use an effective operator formalism, where, one eliminates the excited state manifold such that the dynamics involves only the lower states with effective decay rates, detuning and couplings as prescribed in Ref.[1]. To study the scattering of photons inside the waveguide, we adopt an input-output formalism in the Heisenberg picture, for the field mode operators

$$\hat{a}^f_o(\mathrm{z},t) = \hat{a}^f_{\rm in}(\mathrm{z}-v_g t) + i\sum_{\rm mm'} e^{-i\omega_{\rm mm'}(\mathrm{z'}-\mathrm{z})/v_g}\rho_{\rm mm'}(t)\left[\zeta^{ff}_{\rm m'm}\hat{a}^f_{\rm in}(\mathrm{z}-v_g t) + e^{-2ik_0\mathrm{z'}}\zeta^{fb}_{\rm m'm}\hat{a}^b_{\rm in}(\tilde{\mathrm{z}}+v_g t)\right], \tag{S9}$$

$$\hat{a}^b_o(\mathrm{z},t) = \hat{a}^b_{\rm in}(\mathrm{z}+v_g t) + i\sum_{\rm mm'} e^{i\omega_{\rm mm'}(\mathrm{z'}-\mathrm{z})/v_g}\rho_{\rm mm'}(t)\left[\zeta^{bb}_{\rm m'm}\hat{a}^b_{\rm in}(\mathrm{z}+v_g t) + e^{2ik_0\mathrm{z'}}\zeta^{bf}_{\rm m'm}\hat{a}^f_{\rm in}(\tilde{\mathrm{z}}-v_g t)\right], \tag{S10}$$

where the superscripts $f(b)$ stands for the forward (backward) travelling wave, $\hat{a}_o$ gives the outgoing photon, $\hat{a}_{\rm in}$ is the incoming photon annihilation operator, $\tilde{\mathrm{z}} = (2\mathrm{z'} - \mathrm{z})$ while z′ and z are the position of the scatterer and observation respectively. For the group velocity of the photon wave-packet inside the waveguide v_g, similar dispersion in the forward and backward directions is assumed, and m, m′ are the indices corresponding to all possible initial and final states (attained after the scattering) of the scatterer. The scattering co-efficient, ζ is evaluated to be

$$\zeta^{ij}_{\rm m'm} = \sum_{\rm ee'}\left(\sqrt{\frac{\Gamma^i_{\rm m'e}}{2}}(\mathcal{H}_{\rm nh})^{-1}_{\rm ee'}\sqrt{\frac{\Gamma^j_{\rm e'm}}{2}}\right), \tag{S11}$$

where, $\mathcal{H}_{\rm nh}$ is a non-Hermitian Hamiltonian defined as $\mathcal{H}_{ee'} - \frac{i}{2}\sum_k \mathcal{L}^\dagger_k\mathcal{L}_k$, where $\mathcal{H}_{ee'}$ is part of the Hamiltonian $\mathcal{H}_0$ in the excited state manifold and k stands for the different possible decay paths from the excited state manifold. Here e,e' are indices

corresponding to the excited states of the scatterer, while the rate of scattering into the one-dimensional mode of the optical slot waveguide from the transition $|e\rangle \leftrightarrow |m\rangle$ of the scatterer is given by $\Gamma^{i}_{\mathrm{e'm}} \propto (\mathrm{g}^{i}_{\mathrm{m}}[e' \rightarrow m])^2/v_g$. Note that the above input-output relation derived by generalization of [1] is independent of the kind of scatterers and applies to a multitude of problems involving photon scattering in waveguides [2].

In our coherent scattering scheme, $\mathrm{m} = \mathrm{m}'$ and $\mathrm{e} = \mathrm{e}'$ with $\mathrm{m} \equiv \{|g,\downarrow\rangle, |g,\uparrow\rangle\}$ while $\mathrm{e} \equiv \{|e,\downarrow\rangle, |e,\uparrow\rangle\}$. The reflected photon a^r according to the above input-output relation is then

$$\hat{a}_r(\mathrm{z},t) = \sum_m e^{2ik_0\mathrm{z}'}\rho_{mm}(t)\zeta_{\mathrm{mm}}\hat{a}^{f}_{\mathrm{in}}(\tilde{\mathrm{z}} - v_g t), \tag{S12}$$

where for simplicity we ignore the vacuum noise contribution from modes initially not containing any photons. For scattering with a single photon pulse of carrier frequency ω_{p}, we find that the scattering co-efficient for the transition pathways $|e,\downarrow\rangle \rightarrow |g,\downarrow\rangle \rightarrow |e,\downarrow\rangle$ and $|e,\uparrow\rangle \rightarrow |g,\uparrow\rangle \rightarrow |e,\uparrow\rangle$ to be respectively

$$\zeta_{g,\downarrow} = \left(\frac{\gamma_{1D}}{2}\right)(\Delta - i\gamma/2 - \mathrm{g_c}/2)^{-1}, \qquad \zeta_{g,\uparrow} = \left(\frac{\gamma_{1D}}{2}\right)(\Delta - i\gamma/2 + \mathrm{g_c}/2)^{-1}, \tag{S13}$$

where the detuning is $\Delta = (\omega_m - \omega_{\mathrm{p}})$, $\gamma = \gamma' + \gamma_{1D}$ is total radiative decay rate of the molecular transition with γ' being the decay to the surrounding and $\gamma_{1D} = \Gamma_{\mathrm{e}\uparrow\mathrm{m}\uparrow} = \Gamma_{\mathrm{e}\downarrow\mathrm{m}\downarrow}$, that into the one-dimensional waveguide. Furthermore we find $\rho_{mm}(t) = \rho_{mm}(0) = 1$ from the master equation for the density matrix when the hybrid is initially prepared in the state $|g,\downarrow\rangle$ or $|g,\uparrow\rangle$. The input-output relation then gives the scattered photon depending on the initial state of the qubit $|\downarrow\rangle$ or $|\uparrow\rangle$. From Eq. (S13) we find that resonant scattering occurs by satisfying the resonance conditions $\Delta = \mp \mathrm{g_c}/2$.

We now investigate the coherent scattering dynamics at the charge degeneracy point (sweet spot, $n_g = 1/2$) of the CPB qubit. The qubit states are now represented by an eigen-basis $|\pm\rangle = \frac{1}{\sqrt{2}}(|\uparrow\rangle \pm |\downarrow\rangle)$ of the η_{x} operator which diagonalizes the qubit Hamiltonian $\mathcal{H}_{\mathrm{cp}}$ given in the main text. The corresponding transition frequency ω_{q} is proportional to the Josephson junction energy E_J. The molecule-CPB interaction Hamiltonian at the sweet spot is most conveniently expressed in the diagonalized eigen-basis $|\pm\rangle$. To evaluate the scattering dynamics as before, we choose, a combined molecule-CPB qubit basis $\{|e,+\rangle, |e,-\rangle, |g,+\rangle, |g,-\rangle\}$ and follow the input-ouput formalism for the field mode operators in the same effective operator approach [1]. For the scattering of a single input photon we get corresponding to the qubit state $|\pm\rangle$

$$\hat{a}_{o\pm} = i\zeta_{\pm}\hat{a}_{\mathrm{in}}, \tag{S14}$$

where the scattering amplitudes $\zeta_{\pm}$ are given by,

$$\zeta_{\pm} = \left(\frac{\gamma_{1D}}{2}\right)\frac{\Delta \mp \omega_q - i\frac{\gamma}{2}}{\left(\Delta - i\frac{\gamma}{2}\right)\left(\Delta \mp \omega_q - i\frac{\gamma}{2}\right) - \mathrm{g_c^2}/4}. \tag{S15}$$

From the above expressions we find that in the limit $\gamma \ll \Delta, \omega_{\mathrm{q}}, \mathrm{g_c}$ and $\mathrm{g_c} \ll \omega_{\mathrm{q}}$ the resonance condition for scattering of an incoming photon is $\Delta = \mp \mathrm{g_c^2}/4\omega_{\mathrm{q}}$. Resolving the resonance line for the values of $\mathrm{g_c}$ and ω_q mentioned in the text is not feasible. Hence in this case, we find the difference in the probability of scattering defined as $P_{scatt} \simeq |\zeta_+|^2 - |\zeta_-|^2$ evaluated to the second order to be

$$P_{scatt} \simeq \left(\frac{\gamma_{1D}}{\gamma}\right)^2\left(\frac{\mathrm{g_c^2}}{\omega_{\mathrm{q}}\gamma}\right), \tag{S16}$$

where, we have assumed $\omega_{cp} \gg g_c$ to get the above simple analytical form. For parameters $\gamma_{1D}/\gamma = 0.1, \gamma \simeq 2\pi \times 20$ MHz, $\omega_{\mathrm{q}} = 2\pi \times 10$ GHz and $\mathrm{g_c} \simeq 2\pi \times 80$ MHz as mentioned in the main text, we get $P_{scatt} \sim 10^{-4}$. This is small but still detectable as we are in principle not restricted in photon flux, given the fact that we do not probe the CPB qubit, but rather the molecule with light. Thus with suitable filtering (i.e. building an interferometer around the system) one in 10^4 photons will give rise to a click in a detector if the CPB is in one state and not the other. To suppress decoherence from the light field, it will however be desirable to work at lower light levels and we therefore consider the Raman scheme below.

RAMAN SCATTERING SCHEME

In this scheme we consider two molecules inside the slot-waveguide coupled to each other via optical dipole-dipole interaction. The qubit is assumed to be located near a pair of such dipole coupled molecules and is operated at the charge degeneracy point. The combination of two molecules and the qubit now represent the hybrid structure. The free energy part of the Hamiltonian of such a hybrid is similar to the single molecule case with $\mathcal{H}_{\mathrm{m}} \rightarrow \sum_{\mathrm{k}} \mathcal{H}^{(\mathrm{k})}_{\mathrm{m}}$ where the superscript $k = 1, 2$ denotes the two molecules. The interaction Hamiltonian is in this case a sum of contributions from three different physical processes namely

dipole-dipole interaction $\mathcal{H}_{\rm dd}$, molecule-qubit interaction $\sum_k \mathcal{H}^{\rm I}_{\rm mq,k}$, and molecule-light interaction $\sum_k \mathcal{H}^{\rm I}_{\rm ml,k}$. Following Eq. (S7) and Eq. (S8) these can be written

$$\mathcal{H}_{\rm I} = \mathcal{H}_{\rm dd} + \mathcal{H}^{\rm I}_{\rm ml,k} + \mathcal{H}^{\rm I}_{\rm mq,k} \,,$$

$$\mathcal{H}_{\rm dd} = \hbar {\rm V}(\sigma_1^+\sigma_2^- + \sigma_2^+\sigma_1^-) \,, \tag{S17}$$

$$\mathcal{H}^{\rm I}_{\rm ml,k} = \frac{\hbar {\rm g}_{\rm m_k}}{2}\sigma_{\rm k}^+\hat{a}e^{i[kr_{\rm k}-\omega_{\rm p}t]} + \frac{\hbar {\rm g}_{\rm m_k}}{2}\hat{a}^\dagger\sigma_{\rm k}^- e^{-[ikr_{\rm k}-\omega_{\rm p}t]} \,, \tag{S18}$$

$$\mathcal{H}^{\rm I}_{\rm mq,k} = \frac{\hbar {\rm g}_{\rm c_k}}{4}\eta_{\rm k}^{\rm z}\otimes(\sigma_{\rm k}^{\rm z}+\mathbb{I}) \,, \tag{S19}$$

where $\rm g_{m_k}$ and $\rm g_{c_k}$ are the coupling strength of the $\rm k^{th}$ molecule to the incoming light and the CPB qubit respectively. The combined basis of the molecule-CPB qubit hybrid can be written as $\{|e_1,e_2\rangle\otimes|\pm\rangle, |S\rangle\otimes|\pm\rangle, |A\rangle\otimes|\pm\rangle, |g_1,g_2\rangle\otimes|\pm\rangle\}$. Here the index $1,2$ corresponds to the molecule and $|\pm\rangle$ are the qubit eigenstates at the energy degeneracy point while, the states $|S\rangle = \beta_1|e_1g_2\rangle + \beta_2|g_1e_2\rangle$ and $|A\rangle = \beta_1'|e_1g_2\rangle + \beta_2'|g_1e_2\rangle$ are the eigen-states of the Hamiltonian $\mathcal{H}_{\rm dd}$ with the co-efficients,

$$\beta_1 = \beta_2' = \sqrt{\frac{1}{2}\left(1+\frac{\delta_0}{\sqrt{4{\rm V}^2+\delta_0^2}}\right)} \,, \qquad \beta_1' = \beta_2 = \sqrt{\frac{1}{2}\left(1-\frac{\delta_0}{\sqrt{4{\rm V}^2+\delta_0^2}}\right)} \,. \tag{S20}$$

Here, $\delta_0 = (\omega_{\rm m_1} - \omega_{\rm m_2})$, while the co-efficients satisfy $(\beta_1^2+\beta_2^2) = (\beta_1'^2+\beta_2'^2) = 1$, $\beta_1\beta_2 = \beta_1'\beta_2' = {\rm V}/\sqrt{4{\rm V}^2+\delta_0^2}$, $(\beta_1^2-\beta_2^2) = (\beta_2'^2-\beta_1'^2) = \delta_0/\sqrt{4{\rm V}^2+\delta_0^2}$. We consider the incoming light pulse interacting with the molecules to be quite weak (single to few photons). Hence, two photon processes leading to excitation to the state $|e_1,e_2\rangle$ can be neglected from the scattering dynamics. Thus, the basis states of the hybrid is restricted to $\{|S\rangle\otimes|\pm\rangle, |A\rangle\otimes|\pm\rangle, |g_1,g_2\rangle\otimes|\pm\rangle\}$ as shown in Fig (S4).

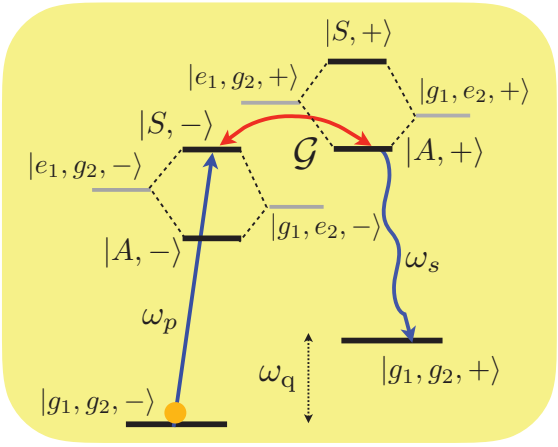

FIG. S4. Schematic of the energy levels in the molecule-SC qubit hybrid for the Raman scattering process. The molecular levels $|e_1g_2\rangle$ and $|g_1e_2\rangle$ are hybridized by the dipole-dipole interaction between the molecules to form the dressed states $|A\rangle$ and $|S\rangle$. The separation of these dressed states can be tuned into resonance with the qubit frequency $\omega_{\rm q}$ (the energy separation between the ground states). Scattering of a photon of frequency $\omega_{\rm p}$ along the transition $|g_1,g_2,-\rangle \to |S,-\rangle$ leads to emission of a Stokes photon $\omega_{\rm s}$ along the transition $|A,+\rangle \to |g_1,g_2,+\rangle$ due to resonant coupling among the states $|S,-\rangle \leftrightarrow |A,+\rangle$.

The states $|S,-\rangle$ and $|A,-\rangle$ in Fig.S4 have energies $\pm\mathcal{V} = \pm\frac{1}{2}\sqrt{4V^2+\delta_0^2}$ corresponding to an energy separation of $2\mathcal{V}$ while $|S,\pm\rangle(|A,\pm\rangle)$ are separated by the qubit transition frequency ω_q equal to the ground state seperation. Furthermore, these dressed states have an effective coupling of $\mathcal{G} = ({\rm g_{c_1}} - {\rm g_{c_2}}){\rm V}/\sqrt{4{\rm V}^2+\delta_0^2}$ among them. For a dipolar interaction strength $V < \omega_{\rm q}$, it is possible to vary the frequency difference among the molecules δ_0 by external field so as to tune the energy difference among the dressed states $2\mathcal{V}$ into resonance with $\omega_{\rm q}$. This resonance condition allows the exchange of energy between the qubit and the excited manifold of the molecules which thereby enables the Raman transition $|g_1,g_2,-\rangle \to |S,-\rangle \to |A,+\rangle \to |g_1,g_2,+\rangle$ when the hybrid interacts with an incoming photon resonant to the transition $|g_1,g_2,-\rangle \to |S,-\rangle$. This process is illustrated in Fig. S4. However, for big δ_0 the coupling among the dressed state becomes weak and one thus needs to strike a balance between

δ_0 and V when selecting two such molecule. For the hybrid structure in the Raman configuration with the above mentioned transition pathways, the non-Hermitian Hamiltonian in the basis $\{|S,\pm\rangle, |A,\pm\rangle\}$ is

$$\mathcal{H}_{\text{nh}}^{(RS)} = \begin{pmatrix} \mathcal{V}+\Delta+\omega_q-\frac{i\Gamma_s}{2} & \frac{\mathcal{G}_1}{2} & -\frac{i\Gamma_{as}}{2} & \mathcal{G} \\ \frac{\mathcal{G}_s}{2} & \mathcal{V}+\Delta-\frac{i\Gamma_s}{2} & \mathcal{G} & -\frac{i\Gamma_{as}}{2} \\ -\frac{i\Gamma_{as}}{2} & \mathcal{G} & -\mathcal{V}+\Delta+\omega_q-\frac{i\Gamma_a}{2} & \frac{\mathcal{G}_a}{2} \\ \mathcal{G} & -\frac{i\Gamma_{as}}{2} & \frac{\mathcal{G}_a}{2} & -\mathcal{V}+\Delta-\frac{i\Gamma_a}{2} \end{pmatrix}, \tag{S21}$$

while that for scattering along the inverse transition pathway $|g_1,g_2,+\rangle \to |A,+\rangle \to |S,-\rangle \to |g_1,g_2,-\rangle$ is

$$\mathcal{H}_{\text{nh}}^{(IS)} = \begin{pmatrix} \mathcal{V}+\Delta-\frac{i\Gamma_s}{2} & \frac{\mathcal{G}_1}{2} & -\frac{i\Gamma_{as}}{2} & \mathcal{G} \\ \frac{\mathcal{G}_1}{2} & \mathcal{V}+\Delta-\omega_q-\frac{i\Gamma_s}{2} & \mathcal{G} & -\frac{i\Gamma_{as}}{2} \\ -\frac{i\Gamma_{as}}{2} & \mathcal{G} & -\mathcal{V}+\Delta-\frac{i\Gamma_a}{2} & \frac{\mathcal{G}_2}{2} \\ \mathcal{G} & -\frac{i\Gamma_{as}}{2} & \frac{\mathcal{G}_2}{2} & -\mathcal{V}+\Delta-\omega_q-\frac{i\Gamma_a}{2} \end{pmatrix}, \tag{S22}$$

where, $\Gamma_{as} = \gamma_c\frac{\delta_0}{\sqrt{4V^2+\delta_0^2}}, \Gamma_s = \gamma + 2\gamma_c\frac{V}{\sqrt{4V^2+\delta_0^2}}, \Gamma_a = \gamma - 2\gamma_c\frac{V}{\sqrt{4V^2+\delta_0^2}}, \mathcal{G}_1 = \frac{1}{2}\left(\text{g}_{\text{c}_1} + \text{g}_{\text{c}_2} + \frac{\delta_0(g_1-g_2)}{\sqrt{4V^2+\delta_0^2}}\right)$, $\mathcal{G}_2 = \frac{1}{2}\left(\text{g}_{\text{c}_1} + \text{g}_{\text{c}_2} - \frac{\delta_0(g_1-g_2)}{\sqrt{4V^2+\delta_0^2}}\right)$ and we have assumed the total decay rate of each emitter ($\gamma_{k=A,B} = \gamma = \gamma_{1D} + \gamma_k^i + \gamma_c$) to be equal. Here γ_k^i is the intrinsic decay of the kth emitter and γ_c is a collective decay rate. These different decay rates reflect that the two molecules can decay both to independent reservoirs giving an intrinsic decay and to a joint reservoir giving a collective decay. For the collective decay we assume that possible energy shifts due to the coupling to the collective reservoir are included in the dipole interaction V. Furthermore for simplicity we assume that the two molecules have the same relative phase in their interaction with the waveguide and the common reservoir. We invoke two different Hamiltonian for the two different transitions pathways, because the initial states have different energies and thus different effective detunings [1]. From the central block of Eq. (S20) and (S21) that involves the $|S,-\rangle \to |A,+\rangle$ and $|A,+\rangle \to |S,-\rangle$ respectively, it is clear that the resonance condition for scattering along the two paths is quite different. Thus a certain choice of the resonance condition will enhanced one transition pathway while suppressing the other.

To describe the scattering dynamics we assume that the waveguide is semi-infinite and single sided. The input-output relations Eq. (S9) and Eq. (S10), then following Ref.[3] reduces to

$$\hat{a}_o(\text{z},t) = \hat{a}_{\text{in}}(\text{z}-v_g t) + i\sum_{\text{m}} e^{-i\omega_{\text{mm}'}(z'-z)/v_g}\rho_{\text{mm}'}(t)\zeta_{\text{mm}'}\hat{a}_{\text{in}}(\text{z}-v_g t), \tag{S23}$$

with now $\Gamma_{\text{em}}/2 \to \Gamma_{\text{em}}$. To evaluate the density matrix elements $\rho_{\text{mm}'}$ appearing in the above equation, for the process $|g,-\rangle \to |S,-\rangle \to |A,+\rangle \to |g,+\rangle$ we use the master equation derived in the effective operator formalism [1]

$$\dot{\hat{\rho}} = :i\left[H_{eff},\hat{\rho}\right] - \frac{1}{2}\sum_k\left(\mathcal{L}_{eff}^{k\dagger}\mathcal{L}_{eff}^k\hat{\rho} + \hat{\rho}\mathcal{L}_{eff}^{k\dagger}\mathcal{L}_{eff}^k\right) + \sum_k \mathcal{L}_{eff}^k\hat{\rho}\mathcal{L}_{eff}^{k\dagger}:, \tag{S24}$$

where : ..... : denotes normal ordering. The effective Hamiltonian is written

$$\begin{aligned} H_{eff} = &\frac{1}{2}\left(\text{g}_{\text{m}_1}\beta_2' + \text{g}_{\text{m}_2}\beta_1'\right)^2\left[\left(\mathcal{H}_{\text{nh}}^{RS}\right)_{22}^{-1} + \left(\mathcal{H}_{\text{nh}}^{RS\dagger}\right)_{22}^{-1}\right]|1\rangle\langle 1|\hat{a}^\dagger\hat{a} \\ &+ \frac{1}{2}\left(\text{g}_{\text{m}_1}\beta_2 - \text{g}_{\text{m}_2}\beta_1\right)^2\left[\left(\mathcal{H}_{\text{nh}}^{IS}\right)_{33}^{-1} + \left(\mathcal{H}_{\text{nh}}^{IS\dagger}\right)_{33}^{-1}\right]|4\rangle\langle 4|\hat{a}^\dagger\hat{a}, \end{aligned} \tag{S25}$$

where we have introduced the convention $|1\rangle = |g_1,g_2,-\rangle$, $|2\rangle = |S,-\rangle$, $|3\rangle = |A,+\rangle$ and $|4\rangle = |g_1,g_2,+\rangle$ that will be used in all further calculations. The effective Lindbald operators are

$$\mathcal{L}_{eff}^k = \mathcal{L}^k\left[\left(\mathcal{H}_{\text{nh}}^{RS}\right)^{-1} + \left(\mathcal{H}_{\text{nh}}^{IS}\right)^{-1}\right]V_+. \tag{S26}$$

Here, $\mathcal{L}^k = \mathcal{L}_1^{\gamma^i} + \mathcal{L}_2^{\gamma^i} + \mathcal{L}^{\gamma_{1D}+\gamma_c}$ and

$$\begin{aligned} V_+ = &\hbar(\text{g}_{\text{m}_1}\beta_2' + \text{g}_{\text{m}_2}\beta_1')|2\rangle\langle 1|\hat{a}e^{i\Delta t} + \hbar(\text{g}_{\text{m}_1}\beta_2 - \text{g}_{\text{m}_2}\beta_1)|3\rangle\langle 4|\hat{a}e^{i(\Delta-\omega_{\text{q}})t} \\ &+ \hbar(\text{g}_{\text{m}_1}\beta_2' + \text{g}_{\text{m}_2}\beta_1')|S,+\rangle\langle 4|\hat{a}e^{i\Delta t} + \hbar(\text{g}_{\text{m}_1}\beta_2 - \text{g}_{\text{m}_2}\beta_1)|A,-\rangle\langle 4|\hat{a}e^{i(\Delta-\mathcal{V})t}, \end{aligned} \tag{S27}$$

$$\mathcal{L}_j^{\gamma^i} = \sqrt{\gamma_j^i}\beta_2'\left(|1\rangle\langle 2| + |4\rangle\langle S,+|\right) + \sqrt{\gamma_j^i}\beta_2\left(|4\rangle\langle 3| + |1\rangle\langle A,-|\right), \tag{S28}$$

$$\mathcal{L}^{(\gamma_{1D}+\gamma_c)} = (\gamma_{1D}+\gamma_c)(\beta_2'+\beta_1')\left(|4\rangle\langle S,+| + |1\rangle\langle 2|\right) + (\gamma_{1D}+\gamma_c)(\beta_2-\beta_1)\left(|4\rangle\langle 3| + |1\rangle\langle A,-|\right). \tag{S29}$$

For a single photon input, we find on solving Eq. (S24) that we should use

$$\rho_{11}(t) = \rho_{11}(0), \quad \rho_{44}(t) = \rho_{44}(0),$$
$$\rho_{14}(t) = \rho_{14}(0)e^{i\omega_{14}t}. \tag{S30}$$

when we insert it into Eq. (S23) because of normal ordering (note that the normal ordering formalism used here merely reflect that a single photon can only be scattered once, and hence there is no evolution in the density matrix before the scattering).

The scattering amplitude $\zeta_{\mathrm{m}=1\mathrm{m}'=4}$ is evaluated from Eq. (S11) by finding the relevant inverse of the non-Hermitian Hamiltonian matrix given in Eq. (S21) and (S22). We evaluate these in a moderate coupling limit $\mathrm{g}^2_{\mathrm{c}_{1,2}}/\gamma\omega_{\mathrm{q}} < 1$ as

$$\left[H_{nh}^{(RS)\dagger}\right]^{-1}_{23}\left[H_{nh}^{(RS)}\right]^{-1}_{32} = \frac{16\mathcal{G}^2}{(4\mathcal{G}^2+\Gamma_s\Gamma_a+4[\epsilon_2^2-\epsilon_1^2])^2+4(\Gamma_s[\epsilon_1-\epsilon_2]+\Gamma_a[\epsilon_1+\epsilon_2])^2}, \tag{S31}$$

$$\left[H_{nh}^{(IS)\dagger}\right]^{-1}_{32}\left[H_{nh}^{(IS)}\right]^{-1}_{23} = \frac{(\frac{1}{4}[\epsilon_1+\epsilon_2][8\Gamma_s\mathcal{G}-4\Gamma_{as}\mathcal{G}_1-16\mathcal{G}(\epsilon_1+\epsilon_2)])^2+(\frac{1}{8}\Gamma_s[8\Gamma_s\mathcal{G}-4\Gamma_{as}\mathcal{G}_1-16\mathcal{G}(\epsilon_1+\epsilon_2)])^2}{\omega_{\mathrm{q}}^4(\Gamma_s^2+4[\epsilon_1+\epsilon_2]^2)^2}, \tag{S32}$$

$$\left[H_{nh}^{(RS)\dagger}\right]^{-1}_{22}\left[H_{nh}^{(RS)}\right]^{-1}_{22} = \frac{16(\Gamma_a+2[\epsilon_2-\epsilon_1])^2}{(4\mathcal{G}^2+\Gamma_s\Gamma_a+4[\epsilon_2^2-\epsilon_1^2])^2+4(\Gamma_s[\epsilon_1-\epsilon_2]+\Gamma_a[\epsilon_1+\epsilon_2])^2}, \tag{S33}$$

$$\left[H_{nh}^{(IS)\dagger}\right]^{-1}_{33}\left[H_{nh}^{(IS)}\right]^{-1}_{33} = \frac{(2[\epsilon_1+\epsilon_2][\Gamma_s-2(\epsilon_1+\epsilon_2)])^2+(\Gamma_s[\Gamma_s-2(\epsilon_1+\epsilon_2])^2}{\omega_{\mathrm{q}}^2(\Gamma_s^2+4[\epsilon_1+\epsilon_2]^2)}, \tag{S34}$$

where $\epsilon_1(\epsilon_2)$ is a small variations of $\Delta(\mathcal{V})$, but $\ll \omega_{\mathrm{q}}/2$. The probability of Raman stokes scattering defined as $\mathcal{P}_R = \zeta_{14}\zeta_{41}$ can then be written as $\mathcal{P}_R = (\gamma_{1D}/\gamma)^2\wp_R$, where we find on using Eq. (S31)

$$\wp_R = \left(\frac{\delta_0}{\omega_{\mathrm{q}}}\right)^2\left[\frac{4\mathcal{G}^2}{\Gamma_s^2\Gamma_a^2/4\gamma^2+4\mathcal{G}^2}\right]. \tag{S35}$$

In arriving at the above expression we have used the optimized resonance condition $\Delta = -\omega_{\mathrm{q}}/2+\mathcal{G}, \mathcal{V} = \omega_{\mathrm{q}}/2$ found by putting $\epsilon_1 = \mathcal{G}$ and $\epsilon_2 = 0$. In practise it is difficult to have a perfect single photon source. As such a more realistic solution is to use a weak coherent state. In the following we study scattering of an input weak light pulse represented by a coherent state $|\alpha\rangle$ interacting with the molecule. For our scheme m,m′ corresponds to the levels $|g_1, g_2, -\rangle$ and $|g_1, g_2, +\rangle$. We hence find for the resonant Raman scattering process, the density matrix elements for the corresponding population and coherences as

$$\rho_{11}(t) = \rho_{11}(0)\left\{\frac{\Gamma_R^{'}}{\Gamma_R+\Gamma_R^{'}}+\left(\frac{\Gamma_R}{\Gamma_R+\Gamma_R^{'}}\right)e^{-(\Gamma_R+\Gamma_R^{'})|\alpha|^2t}\right\}+\rho_{44}(0)\left(\frac{\Gamma_R^{'}}{\Gamma_R+\Gamma_R^{'}}\right)(1-e^{-(\Gamma_R+\Gamma_R^{'})|\alpha|^2t}), \tag{S36}$$

$$\rho_{44}(t) = \rho_{44}(0)\left\{\frac{\Gamma_R}{\Gamma_R+\Gamma_R^{'}}+\left(\frac{\Gamma_R^{'}}{\Gamma_R+\Gamma_R^{'}}\right)e^{-(\Gamma_R+\Gamma_R^{'})|\alpha|^2t}\right\}+\rho_{11}(0)\left(\frac{\Gamma_R}{\Gamma_R+\Gamma_R^{'}}\right)(1-e^{-(\Gamma_R+\Gamma_R^{'})|\alpha|^2t}), \tag{S37}$$

$$\rho_{14}(t) = \rho_{14}(0)e^{(i\omega_{14}-\Gamma_{RR'}/2)|\alpha|^2t}, \tag{S38}$$

where

$$\omega_{14} = (\mathrm{g}_{\mathrm{m}_1}\beta_2'+\mathrm{g}_{\mathrm{m}_2}\beta_1')^2\left[H_{nh}^{(RS)\dagger}\right]^{-1}_{22}\left[H_{nh}^{(RS)}\right]^{-1}_{22}+(\mathrm{g}_{\mathrm{m}_1}\beta_2'-\mathrm{g}_{\mathrm{m}_2}\beta_1')^2\left[H_{nh}^{(IS)\dagger}\right]^{-1}_{33}\left[H_{nh}^{(IS)}\right]^{-1}_{33}, \tag{S39}$$

$$\Gamma_R = \left[(\gamma_{1D}+\gamma_c)(\beta_2-\beta_1)^2+\gamma_1^i\beta_2^2+\gamma_2^i\beta_1^2\right](\mathrm{g}_{\mathrm{m}_1}\beta_2'+\mathrm{g}_{\mathrm{m}_2}\beta_1')^2\left[H_{nh}^{(RS)\dagger}\right]^{-1}_{23}\left[H_{nh}^{(RS)}\right]^{-1}_{32}, \tag{S40}$$

$$\Gamma_R^{'} = \left[(\gamma_{1D}+\gamma_c)(\beta_2^{'}+\beta_1^{'})^2+\gamma_1^i\beta_2^{'2}+\gamma_2^i\beta_1^{'2}\right](\mathrm{g}_{\mathrm{m}_1}\beta_2-\mathrm{g}_{\mathrm{m}_2}\beta_1)^2\left[H_{nh}^{(IS)\dagger}\right]^{-1}_{32}\left[H_{nh}^{(IS)}\right]^{-1}_{23}, \tag{S41}$$

$$\begin{aligned}\Gamma_{RR'} = &\left[(\gamma_{1D}+\gamma_c)(\beta_2'+\beta_1')^2+\gamma_1^i\beta_2^{'2}+\gamma_2^i\beta_2^{'1}\right](\mathrm{g}_{\mathrm{m}_1}\beta_2'+\mathrm{g}_{\mathrm{m}_2}\beta_1')^2\left[H_{nh}^{(RS)\dagger}\right]^{-1}_{22}\left[H_{nh}^{(RS)}\right]^{-1}_{22}\\ &+\left[(\gamma_{1D}+\gamma_c)(\beta_2'-\beta_1')^2+\gamma_1^i\beta_2^{'2}+\gamma_2^i\beta_2^{'1}\right](\mathrm{g}_{\mathrm{m}_1}\beta_2'-\mathrm{g}_{\mathrm{m}_2}\beta_1')^2\left[H_{nh}^{(IS)\dagger}\right]^{-1}_{33}\left[H_{nh}^{(IS)}\right]^{-1}_{33}+\Gamma_R+\Gamma_R^{'}.\end{aligned} \tag{S42}$$

The right hand side of Eq. (S40) can be separated into two parts, one proportional to the probability of Raman scattering $\mathcal{P}_R$ into the waveguide while the other is proportional to the probability of Raman scattering $\mathcal{P}_{RO}$ to the outside which include processes where a photon is lost after scattering. On using Eqs. (S31) and (S32) in Eqs. (S40) and (S41), we find the probability of Raman

Stokes scattering into the waveguide mode to be $\mathcal{P}_R = (\gamma_{1D}/\gamma)^2 \wp_R$ where $\wp_R$ is given in Eq. (S35). The Raman scattering to modes other than the waveguide is found to be

$$\mathcal{P}_{RO} = \left(\frac{\gamma_{1D}}{\gamma}\right)\left(\frac{\gamma_c}{\gamma}\right)\left(\frac{\delta_0}{\omega_{\rm q}}\right)^2 \left[\frac{2\mathcal{G}^2}{\Gamma_s^2\Gamma_a^2/4\gamma^2 + 4\mathcal{G}^2}\right] + \left(\frac{\gamma_{1D}}{\gamma}\right)\left(\frac{\gamma^i}{\gamma}\right)\left(1 + \frac{2V}{\omega_{\rm q}}\right)\left[\frac{2\mathcal{G}^2}{\Gamma_s^2\Gamma_a^2/4\gamma^2 + 4\mathcal{G}^2}\right]. \tag{S43}$$

Here we have assumed $\gamma_1^i = \gamma_2^i$. On evaluating (S41) we find that,

$$\Gamma_R^{'} = \left[\left(\frac{\gamma_{1D}}{\gamma}\right)^2\left(\frac{\delta_0}{\omega_{\rm q}}\right)^2 + \left(\frac{\gamma_{1D}}{\gamma}\right)\left(\frac{\gamma_c}{\gamma}\right)\left(\frac{\delta_0}{\omega_{\rm q}}\right)^2 + \left(\frac{\gamma_{1D}}{\gamma}\right)\left(\frac{\gamma^i}{\gamma}\right)\left(1 - \frac{2\rm V}{\omega_{\rm q}}\right)\right]\left(\frac{\mathcal{G}^2}{\gamma\omega_{\rm q}^2}\right)^2 \frac{\left(1 + \Gamma_{as}\mathcal{G}_1/4\mathcal{G}^2 - \Gamma_s/2\mathcal{G}\right)^2}{\Gamma_s^2/\gamma^2 + 4\mathcal{G}^2/\gamma^2}. \tag{S44}$$

After some algebra we get in the leading order, $\Gamma_R^{'}/\Gamma_R \propto (\mathcal{G}\gamma)^2/\omega_{\rm q}^4$. Hence under the chosen resonance condition the Raman stokes process dominates over the inverse Raman process. This can also be understood from the above matrices in Eq. (S21) and (S22), where one finds from the inverse of the elements of the central blocks that the transition $|S,-\rangle \rightarrow |A,+\rangle$ dominates the scattering process for the above mention set of resonance condition. For all further use of the Raman scattering we will thus neglect $\Gamma_R^{'}$.

ENTANGLEMENT GENERATION BETWEEN A HYBRID AND PHOTON

We first investigate entanglement between a stationary qubit and a photonic qubit by entangling the hybrid and a single photon in an interferometric setup via post-selection of scattering event. Similar scheme has been shown to achieve a perfect gate no matter how bad the light-matter coupling is [4]. As we will show in the following we can achieve perfect operation similar to what was reported in [4]. The schematic of the entangling mechanism is depicted in Fig. S5 . The hybrid considered to be in the Raman configuration as shown in Fig.S4 forms one arm of the interferometer. Physically the entanglement creation can be understood as follows. An incoming single photon pulse $\hat{a}_{\rm in}$, after passing through the beam splitter BS1 is spatially separated into two components $\hat{a}_1$ and $\hat{a}_2$. The $\hat{a}_2$ component is scattered from the hybrid A resulting in a scattered photon $\hat{a}_{\rm o}^A$. The other component $\hat{a}_1$, travels along the other arm of the interferometer, and gets frequency modulated by the modulator with frequency $\Delta\omega = \omega_{\rm q}$ and also acquires a phase ϕ, while passing through the phase shifter to become $\hat{a}_o^1$. The two output components $\hat{a}_o^A$ and $\hat{a}_o^1$ then interfere at the beam splitter BS2 coherently to form the detector mode operators $\hat{d}_\pm^o$. The photons at the two output ports of the BS2 are collected by the single photon detectors $\rm D_\pm$. If the hybrid is initialized in the state $|g,-\rangle = |g_1, g_2, -\rangle = |1\rangle$, then post-selecting the events where there is scattering, as we shall show below, leads to an entangled state of matter qubit and photonic qubit wriiten as,

$$|\Psi_{\rm s}^+\rangle = \frac{1}{\sqrt{2}}\left(|U_k\rangle|1\rangle + |L_k\rangle|4\rangle\right), \tag{S45}$$

where, U_k and L_k represent respectively a photon reflected from BS1 and a photon which has undergone Raman scattering. For a balanced interferometer, a click on the single photon detectors after the phase Φ have been applied then project the hybrid into a superposition of the lower states $|\Psi^\pm\rangle = \frac{1}{\sqrt{2}}(|1\rangle \pm e^{i\Phi}|4\rangle)$, depending on which of the detectors $D_\pm$ clicks. The post selected dynamics conditioned on the detection of a frequency shifted single photon is thus completely equivalent to the dynamics of a maximally entangled state and allow e.g., the violation of Bell's inequality.

We next mathematically treat the interferometric creation of entanglement and verify it via a Bell inequality violation corresponding to the entangled state $|\Psi_{\rm s}^+\rangle$. For the hybrid prepared initially in the state $|\Psi_{\rm ini}\rangle = |g,-\rangle = |1\rangle$, after scattering a single incoming photon via the Raman process, evolves to some state $|j\rangle$ at a time $t \gg 1/\gamma$ conditioned on detection of a photon at the single photon detectors $D_\pm$. The amplitude of this component is then given by

$$\mathcal{C}_j = \langle j, \emptyset|\hat{d}_+^o(t)U(t)\hat{d}^{\rm in\dagger}|\Psi_{\rm ini}, \emptyset\rangle \tag{S46}$$

Here, the input and output field mode operators $\hat{d}^{\rm in}$ and $\hat{d}_\pm^o$ respectively are defined by,

$$\hat{d}_\pm^o(t) = \frac{1}{\sqrt{2}}\sqrt{\eta}(e^{i\Phi}\hat{a}_o^1(t) \pm \hat{a}_o^A(t)) + \hat{\mathcal{F}} \tag{S47}$$

$$\hat{d}^{\rm in} = \frac{1}{\sqrt{2}}(e^{i\omega_{\rm q}t}\chi\hat{a}_1 + \sqrt{1-\chi^2}\hat{a}_2) \tag{S48}$$

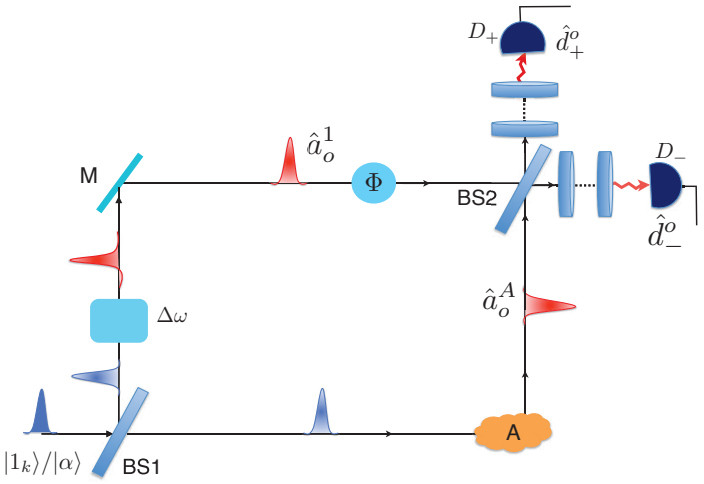

FIG. S5. Interferometric scheme to create entanglement between photons and the hybrid A. The incoming photon pulse after passing through beam splitter BS1 is spatially separated and travels along two arms of the interferometer. One of the component passes through a frequency modulator $\Delta\omega = \omega_q$ and an optical element that introduces an addition phase Φ to interfere at beam splitter BS2 with the other component which undergoes a Raman scattering. The two detectors $D_\pm$ then does a joint measurement of the photon in a basis determined by the beamsplitter and the phase Φ to setup a CHSH inequality verification. Violation of the inequality proves entanglement between the photons and the hybrid emitter A.

where in writing Eq. (S48) we assumed the beam splitter BS1 to be asymmetric with χ as the asymmetric co-efficient, $\hat{\mathcal{F}}$ is the noise operator and η is the photo detection efficiency of the single photon detectors.The exponential describe the modulation done by the modulator, and

$$\begin{aligned}\hat{a}^A_o(t) &= \hat{a}_2 + ie^{-i\omega_q(z_A-z)/v_g}\zeta_{41}\rho_{14}(t)\hat{a}_2,\\ \hat{a}^1_o(t) &= \hat{a}_1\end{aligned} \tag{S49}$$

Furthermore, we assumed a semi-infinite single sided waveguide and have used the input-output relation of Eq. (S23) with ζ_{41} defined in Eq. (S11) while $\rho_{14}(t)$ for a single photon input is given by Eq. (S30).

From Eq. (S46) we can write down the corresponding normalized density matrix elements as,

$$\begin{aligned}\rho^{\pm}_{s_{ij}} &= \frac{\mathrm{Tr}\left(|i\rangle\langle j|\hat{d}^o_\pm(t)U(t)d^{\dagger\mathrm{in}}|\Psi_{\mathrm{ini}},\emptyset\rangle\langle\Psi_{\mathrm{ini}},\emptyset|d^{\mathrm{in}}U^\dagger(t)\hat{d}^{o\dagger}_\pm(t)\right)}{\mathrm{Tr}(\rho^\pm_s)},\\ &= \frac{\langle\Psi_{\mathrm{ini}},\varnothing|\hat{d}^{\mathrm{in}}U^\dagger(t)\hat{d}^{o\dagger}_\pm(t)U(t)U^\dagger(t)|i\rangle\langle j|U(t)U^\dagger(t)\hat{d}^o_\pm(t)U(t)\hat{d}^{\dagger\mathrm{in}}|\Psi_{\mathrm{ini}},\varnothing\rangle}{\mathrm{Tr}(\rho^\pm_s)},\\ &= \frac{\langle\Psi_{\mathrm{ini}},\emptyset|\hat{d}^{\mathrm{in}}\hat{d}^{o\dagger}_{H,\pm}(t)\rho^H_{ij}(t)\hat{d}^0_{H,\pm}(t)\hat{d}^{in,\dagger}|\Psi_{\mathrm{ini}},\emptyset\rangle}{\mathrm{Tr}(\rho^\pm_s)}.\end{aligned} \tag{S50}$$

Here, Tr_f is the trace over all the field modes and the superscript/subscript H stand for Heisenberg picture. For all later reference we will drop this subscript/superscript with the underlying assumption that all the operator evolution is in the Heisenberg picture. Note that we here conditioned on a single detection at a time t. Since for now we only consider a single incident photon at most a single photon can come out and this provide a complete characterization of the output. On evaluating Eq. (S50) we find the components of $\rho^\pm_s$ to be

$$\rho^\pm_{s,11} = \frac{1}{2}, \qquad \rho^\pm_{s,44} = \frac{1}{2}, \qquad \rho^\pm_{s,14} = \mp\frac{1}{2}ie^{-i\omega_q T}e^{i\Phi}, \tag{S51}$$

where we assume the interferometer to be balanced with all other phases absorbed. Note that after the detection at time t, the density matrix should be propagated to the final time T. Combining this with the phase evolution appearing in (S48) leads to a total relative phase of $e^{-i\omega_q T}$ as seen in the above equation. We will omit this phase for all further calculations as it merely reflect the fact that the density matrix is not in the interaction picture with respect to $\mathcal{H}_0$.

To check the quantum correlation among the hybrid and the photon and thereby the entanglement of the state $|\Psi_{\mathrm{ent}}\rangle$ we next consider a Bell -CHSH inequality [5, 6] violation measurement involving single photon detection at the detectors $\mathrm{D}_\pm$. Projecting

the density matrix $\rho_{\rm s}^{\pm}$ on the state $|\Psi_m^{\pm}\rangle = \frac{1}{\sqrt{2}}\left(|1\rangle \pm e^{i\Psi}|4\rangle\right)$ in the measurement basis characterized by the angle Ψ we find the joint probability of qubit detection and photodetection at the detectors $\mathrm{D}_{\pm}$ given by $P_{\pm\pm}$ to be

$$\begin{aligned} P_{++} = P_{--} &= \frac{1}{2}\cdot\frac{1}{2}\left[1+\sin\left(\Psi-\Phi\right)\right], \\ P_{+-} = P_{-+} &= \frac{1}{2}\cdot\frac{1}{2}\left[1-\sin\left(\Psi-\Phi\right)\right]. \end{aligned} \tag{S52}$$

Here, the first and second subscript of P stands for the photon detection by a respective detector and projection of the hybrid to either of the states $|\Psi_{\rm s}^{\pm}\rangle$. The measurement outcome for certain choice of phases can then be written in spirit of the Bell inequality as,

$$E(\Psi_{\rm a},\theta_{\rm b}) = \frac{P_{++}+P_{--}-P_{+-}-P_{-+}}{P_{++}+P_{--}+P_{+-}+P_{-+}} = \sin\left(\Psi_{\rm a}-\Phi_{\rm b}\right). \tag{S53}$$

The Bell inequality violation parameter can then be defined as

$$S = E(\Psi_{\rm a},\theta_{\rm b}) - E(\Psi_{\rm a},\theta_{\rm b'}) + E(\Psi_{\rm a'},\theta_{\rm b}) + E(\Psi_{\rm a'},\theta'_{\rm b}), \tag{S54}$$

and we get a maximal violation $S = 2\sqrt{2}$ for the following set of phase angles $\{\Psi_{\rm a},\Psi_{\rm a'},\Phi_{\rm b},\Phi_{\rm b'}\} = \{\pi/4, 3\pi/4, 0, \pi/2\}$. The corresponding success probability is given by

$$\begin{aligned} P_{\rm suc}^{(1)} &= \langle\Psi_{\rm ini},\emptyset|\hat{d}^{\rm in}\hat{d}_{\pm}^{o\dagger}(t)\hat{d}_{\pm}^{o}(t)\hat{d}^{\rm in\dagger}|\Psi_{\rm ini},\emptyset\rangle \\ &= 2\eta\zeta_{41}\zeta_{41}^{\dagger}(1-\chi^2) \end{aligned} \tag{S55}$$

where, $\zeta_{41}\zeta_{41}^{\dagger} = \left(\sqrt{\gamma_{1D}^{43}}(H_{nh}^{(2)})_{32}^{-1}\sqrt{\gamma_{1D}^{21}}\right)\left(\sqrt{\gamma_{1D}^{12}}(H_{nh}^{(2)\dagger})_{23}^{-1}\sqrt{\gamma_{1D}^{34}}\right)$. In writing the above expression for success probability we add contribution from both the detectors as they both give the desired outcome. On using the resonance conditions along with Eq. (S31) in Eq. (S55) we get

$$P_{\rm suc}^{(1)} = 2\eta\mathcal{P}_R(1-\chi^2), \tag{S56}$$

where $\mathcal{P}_R$ is given in Eq. (S35).

If the incoming photon pulse $\hat{a}_{\rm in}$ is assumed to be in a coherent state $|\alpha\rangle$ then Eq.(S50) becomes,

$$\rho_{{\rm s}_{ij}}^{(\pm)} = \frac{\langle\Psi_{\rm ini},\alpha|\hat{d}_{\pm}^{o\dagger}(t)\rho_{ij}^{\pm}(t)\hat{d}_{\pm}^{o}(t)|\Psi_{\rm ini},\alpha\rangle}{\mathrm{Tr}(\rho_{\rm s}^{\pm})}, \tag{S57}$$

In Eq. (S46) we conditioned on having clicks at a certain time t, represented by the operators $d_{\pm}^{o}$. Experimentally one would however, only consider the first click which arrive at the detector. This makes no difference above where only a single photon is involved in the process. With an incident coherent state a more correct description would be to include in Eq. (S57) the requirement that there is no photon detected before the time t. Since we mainly consider the the limit of low (γ_{1D}/γ), the probability of having two detection events in the time interval is negligible and the simple description in Eq. (S57) is sufficient. Following the procedure as discussed in details for the single photon input pulse, and considering $\rho_{{\rm s}_{ij}}^{(\pm)}(t)$ with the time evolution of the matrix elements given by Eqs. (S36) - (S38) we arrive at a CHSH measurement outcome of

$$E(\Psi_{\rm a},\theta_{\rm b}) = \frac{P_{++}+P_{--}-P_{+-}-P_{-+}}{P_{++}+P_{--}+P_{+-}+P_{-+}} = \left[\frac{2e^{-(\mathcal{P}_R+\mathcal{P}_{RO})|\alpha|^2 t}}{1+e^{-(\mathcal{P}_R+\mathcal{P}_{RO})|\alpha|^2 t}}\right]\sin\left(\Psi_{\rm a}-\Phi_{\rm b}\right), \tag{S58}$$

Substituting this measurement outcome into the Bell inequality of Eq. (S54) then gives us the violation parameter as

$$S = 2\sqrt{2}\left[\frac{2e^{-(\mathcal{P}_R+\mathcal{P}_{RO})\bar{n}}}{1+e^{-2(\mathcal{P}_R+\mathcal{P}_{RO})\bar{n}}}\right], \tag{S59}$$

where $\bar{n}$ is the mean number of photons involved in the scattering process. The corresponding success probability is given by

$$\begin{aligned} P_{\rm suc}^{(c)} &= \int_0^T dt\langle\Psi_{\rm ini},\alpha|\hat{d}_{\pm}^{o\dagger}(t)\hat{d}_{\pm}^{o}(t)|\Psi_{\rm ini},\alpha\rangle, \\ &= \eta\zeta_{41}\zeta_{41}^{\dagger}(1-\chi^2)\left(\frac{1-e^{-2\bar{n}\Gamma_R}}{2\Gamma_R}\right), \\ P_{\rm suc}^{(c)} &= \frac{1}{2}P_{\rm suc}^{(1)}\left(\frac{1-e^{-2\bar{n}[\mathcal{P}_R+\mathcal{P}_{RO}]}}{\mathcal{P}_R+\mathcal{P}_{RO}}\right) \end{aligned} \tag{S60}$$

We plot Eqs. (S59) and (S60) in Fig. 3(c) in the main text for an asymmetry co-efficient of 70%.

ENTANGLEMENT GENERATION BETWEEN TWO HYBRIDS

To entangled two hybrids we consider a similar interferometric setup to that shown schematically in Fig. S5(a) but now with hybrids A and B in both the arms of the interferometer and BS1 is a $50-50$ beam splitter as shown in Fig. 3(a) of the main text. The physics behind the generation of entanglement has been detailed in the main text. Here we concentrate on the mathematical treatment and focus on evaluating the fidelity and success probabililty of the entangled state. The hybrids are initially prepared in the state $|\Psi_{\rm ini}\rangle = |g,-\rangle_{\rm A}\otimes|g,-\rangle_{\rm B} = |1\rangle_{\rm A}|1\rangle_{\rm B}$. Due to Raman scattering of a single photon the hybrids evolves to the entangled state $|\Psi_{\pm}\rangle$, conditioned on the detection of a photon in either of the detectors $\rm D_{\pm}$. The fidelity $F = \langle\Psi_{\pm}|\rho^{\pm}_{\rm AB}|\Psi_{\pm}\rangle$ of the state $|\Psi_{\pm}\rangle$ can be evaluated by finding the time evolved density matrix components,

$$\rho^{\pm}_{{\rm AB}_{ij}} = \frac{\langle\Psi_{\rm ini},\emptyset|\hat{d}^{in}\hat{d}^{o\dagger}_{\pm}(t)\rho^{\pm}_{ij}(t)\hat{d}^{o}_{\pm}(t)\hat{d}^{in\dagger}|\Psi_{\rm ini},\emptyset\rangle}{{\rm Tr}(\rho^{\pm}_{\rm AB})}, \tag{S61}$$

where the input and output field mode operators are defined respectively by

$$\begin{aligned}\hat{d}^{o}_{\pm}(t) &= \frac{1}{\sqrt{2}}\sqrt{\eta}(\hat{a}^{\rm A}_{o}(t)\pm\hat{a}^{\rm B}_{o}(t)) + \mathcal{F},\\ \hat{d}^{\rm in} &= \frac{1}{\sqrt{2}}(\hat{a}^{\rm A}_{1}+\hat{a}^{\rm B}_{1}).\end{aligned} \tag{S62}$$

The input-output relation of Eq. (S23) gives

$$\hat{a}^{j}_{o}(t) = \hat{a}^{j}_{1} + ie^{-i\omega_{\rm q}(z_j-z)/v_g}\zeta^{j}_{41}\rho^{j}_{14}(t)\hat{a}^{j}_{1}, \tag{S63}$$

where, ζ_{41} can be evaluated following Eq. (S11). Substituting Eq. (S62) in Eq. (S61) and on using Eq. (S63) and considering identical characteristics for the hybrid we find

$$\rho^{\pm}_{{\rm AB}_{11}} = \frac{1}{2}, \qquad \rho^{\pm}_{{\rm AB}_{44}} = \frac{1}{2}, \qquad \rho^{\pm}_{{\rm AB}_{41,14}} = \pm\frac{1}{2}. \tag{S64}$$

For detection at D_{-}- the quality of the entangled state is characterized by the fidelity $F = \langle\Psi_{-}|\rho^{-}_{AB}|\Psi_{-}\rangle$ which attains the ideal value of $F=1$. The corresponding success probability is given by

$$\begin{aligned}P^{(1)}_{\rm suc} &= \langle\Psi_{\rm ini},\emptyset|\hat{d}^{\rm in}\hat{d}^{o\dagger}_{-}(t)\hat{d}^{o}_{-}(t)\hat{d}^{\rm in\dagger}|\Psi_{\rm ini},\emptyset\rangle\\ &= \frac{1}{2}\eta\zeta_{41}\zeta^{\dagger}_{41} = \frac{1}{2}\eta\left(\sqrt{\gamma^{43}_{1D}}(H^{(2)}_{nh})^{-1}_{32}\sqrt{\gamma^{21}_{1D}}\right)\left(\sqrt{\gamma^{12}_{1D}}(H^{(2)\dagger}_{nh})^{-1}_{23}\sqrt{\gamma^{34}_{1D}}\right),\end{aligned} \tag{S65}$$

which on using the resonance conditions along with Eq. (S31) gives us

$$P^{(1)}_{\rm suc} = \eta\mathcal{P}_{R}, \tag{S66}$$

where $\mathcal{P}_R$ is given in Eq. (S35). In writing the above expression for success probability we add contribution from both the $\pm$ detectors as they both give the desired outcome.

To get the plot of Fig. 2 in the main text, we express the success probability as a function of the ratio of the dipolar coupling between the molecules and the SC qubit transition frequency $\rm V/\omega_q$, and the couplings of the molecule to the SC qubits $\left(\rm g_{c_1}-g_{c_2}\right)$. By using the resonance conditions for optimization of the the Raman process we can write $\delta^2_0 = \omega^2_{\rm q} - 4{\rm V}^2$. Substituting this into Eq. (S66) the expression for $\mathcal{P}_R$ can be re-written using Eq. (S35),

$$\mathcal{P}_R\left(\gamma/\gamma_{1D}\right)^2 = \frac{16\left(1-4y^2\right)y^2x^2}{16y^2x^2+\left(1-4y^2\left(\frac{\gamma_c}{\gamma}\right)^2\right)^2}, \tag{S67}$$

where $y = \left(\rm g_{c_1}-g_{c_2}\right)/\gamma$ and $x = \rm V/\omega_q$.

If the incoming photon pulse is assumed to be in a coherent state $|\alpha\rangle$, the above treatment for evaluating the fidelity and success probability remains valid with some modifications. The components of the density matrix for the state $|\Psi_{\pm}\rangle$ now becomes,

$$\rho^{\pm}_{{\rm AB}_{ij}} = \frac{\langle\Psi_{\rm ini},\alpha|\hat{d}^{o\dagger}_{\pm}(t)\rho^{\pm}_{ij}(t)\hat{d}^{o}_{\pm}(t)|\Psi_{\rm ini},\alpha\rangle}{{\rm Tr}(\rho^{\pm}_{\rm AB})}. \tag{S68}$$

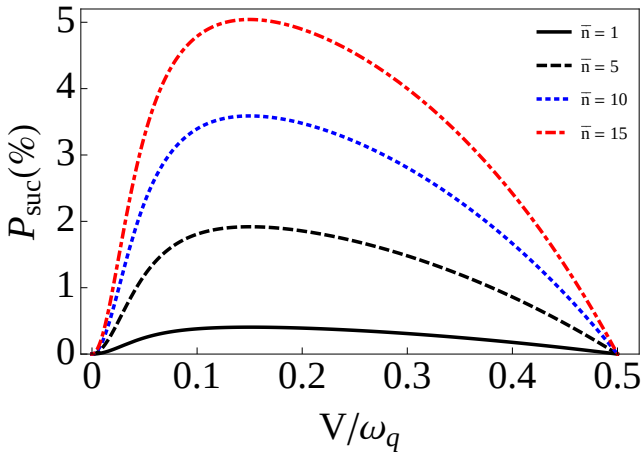

FIG. S6. $P_{\rm suc}$ as a function of $\mathrm{V}/\omega_{\rm q}$ for different values of the mean photon number in the incoming photon pulse. We have assumed $\gamma_c/\gamma = 0.45, \gamma^i/\gamma = 0.45, \gamma_{1D}/\gamma = 0.1$ and $\left(\mathrm{g}_{\mathrm{c}_1} - \mathrm{g}_{\mathrm{c}_2}\right)/\gamma = 5$.

The fidelity $F = \langle\Psi_-|\rho^-_{\rm AB}|\Psi_-\rangle$ and the success probability $P^{(c)}_{\rm suc}$ for the entangled stated $|\Psi_-\rangle$ is in this case

$$F = e^{-\Gamma_R|\alpha|^2 t}; \qquad P^{(c)}_{\rm suc} = \int_0^T dt\, \langle\Psi_{\rm ini}, \alpha|\hat{d}^{o\dagger}_{\pm}(t)\hat{d}^{o}_{\pm}(t)|\Psi_{\rm ini}, \alpha\rangle. \tag{S69}$$

On using the input-output relation and the definition of the output field mode operators we find the success probability under the resonance condition to be

$$P^{(c)}_{\rm suc} = \eta|\alpha|^2\zeta_{41}\zeta^\dagger_{41}\int_0^T dt\, e^{-\Gamma_R|\alpha|^2 t} = \frac{P^{(1)}_{\rm suc}}{\Gamma_R}\left(1 - e^{-\Gamma_R|\alpha|^2 T}\right). \tag{S70}$$

On substituting Eq. (S66) for $P^{(1)}_{\rm suc}$ and Eqs. (S35) and (S43) for Γ_R in the above equation we get the fidelity and success probability as

$$\begin{aligned} F &= 1 - \left(1 + \frac{\mathcal{P}_{RO}}{\mathcal{P}_R}\right)\frac{P^{(c)}_{\rm suc}}{\eta}, \\ &= 1 - \frac{P^{(c)}_{\rm suc}}{\eta} - \frac{1}{2}\left(1 - 2\mathrm{V}/\omega_{\rm q}\right)^{-1}\left[\left(\frac{\gamma_c + \gamma^i}{\gamma}\right) - 2\mathrm{V}/\omega_{\rm q}\left(\frac{\gamma_c}{\gamma}\right)\right]\left(\frac{\gamma}{\gamma_{1D}}\right)\frac{P^{(c)}_{\rm suc}}{\eta}, \end{aligned} \tag{S71}$$

$$P^{(c)}_{\rm suc} = \frac{P^{(1)}_{\rm suc}}{(\mathcal{P}_R + \mathcal{P}_{RO})}\left\{1 - e^{-\bar{n}(\mathcal{P}_R + \mathcal{P}_{RO})}\right\}. \tag{S72}$$

To the lowest order in expansion of the exponential we find $P_{\rm suc} = \bar{n}P^{(1)}_{\rm suc}$. We plot $P^{(c)}_{\rm suc}$ as a function of the ratio between the dipole coupling between the molecules and the SC qubit transition energy $(V/\omega_{\rm q})$ in Fig. S6 for different values of the mean photon number.

We find that the $P^{(c)}_{suc}$ increases significantly with the mean number of photons. As $V/\omega_{\rm q} \to 1/2$, the antisymmetric state $|A\rangle$ in Fig. (S2) becomes decoupled from the dynamics of the rest of the system and hence the probability of Raman scattering vanishes $\mathcal{P}_R \longrightarrow 0$ which thereby leads to vanishing success probability.

[1] F. Reiter, and A. S. Sørensen, Phys. Rev. A, **85**, 032111 (2012).
[2] S. Das, F. Reiter, and A. S. Sørensen, in preparation
[3] D. Witthaut, and A. S. Sørensen, New Journal of Physics, **12** 043052 (2010).
[4] Y. Li, L. Aolita, D. E. Chang, and L. C. Kwek, Phys. Rev. Lett. **109**, 160504 (2012).
[5] J. F. Clauser, M. A. Horne, A. Shimony, and R. A. Holt, Phys. Rev. Lett. **23**, 880 (1969).
[6] A. Aspect, P. Grangier, and G. Roger Phys. Rev. Lett. **47**, 460 (1981).